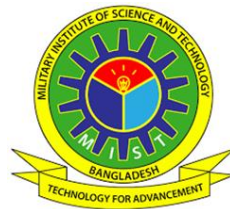


EFFECT OF SOILING ON SOLAR PANELS: IN-FIELD OUTPUT CHARACTERIZATION FOR CLEANING-CYCLE AND ECONOMIC ANALYSIS

MOHAMMAD DIDARUL ISLAM

M.SC ENGINEERING THESIS



**DEPARTMENT OF ELECTRICAL, ELECTRONIC, AND
COMMUNICATION ENGINEERING
MILITARY INSTITUTE OF SCIENCE AND TECHNOLOGY
DHAKA, BANGLADESH**

APRIL 2023

**EFFECT OF SOILING ON SOLAR PANELS: IN-FIELD OUTPUT
CHARACTERIZATION FOR CLEANING-CYCLE AND ECONOMIC
ANALYSIS**

MOHAMMAD DIDARUL ISLAM (SN. 0420160007)

**A Thesis Submitted in Partial Fulfillment of the Requirements for the Degree of Master
of Science in Electrical, Electronic, and Communication Engineering**



**DEPARTMENT OF ELECTRICAL, ELECTRONIC, AND COMMUNICATION
ENGINEERING**

MILITARY INSTITUTE OF SCIENCE AND TECHNOLOGY

DHAKA, BANGLADESH

APRIL 2023

**EFFECT OF SOILING ON SOLAR PANELS: IN-FIELD OUTPUT
CHARACTERIZATION FOR CLEANING-CYCLE AND ECONOMIC
ANALYSIS**

M.Sc. Engineering Thesis

By

MOHAMMAD DIDARUL ISLAM (SN. 0420160007)

Approved as to style and content by the Board of Examination on 13th April 2023:

Dr. Mohammad Ryyan Khan
Associate Professor and Chairperson, Dept. of EEE
East West University

Chairman (Supervisor)
Board of Examination

Lt Col Md Aminul Islam, PhD
Instructor Class 'A', Dept. of EECE
Military Institute of Science and Technology

Member (Co-Supervisor)
Board of Examination

Dr. Md Zunaid Baten
Associate Professor, Dept. of EEE
Bangladesh University of Engineering and Technology

Member (External)
Board of Examination

Dr. Md Golam Mostafa
Professor, Dept. of EECE
Military Institute of Science and Technology

Member (Internal)
Board of Examination

Brig Gen Md Mahfuzul Karim Majumder
Senior Instructor, and Dean, Faculty of ECE
Military Institute of Science and Technology

Member (Ex-Officio)
Board of Examination

Dept. EECE, MIST, Dhaka

EFFECT OF SOILING ON SOLAR PANELS: IN-FIELD OUTPUT CHARACTERIZATION FOR CLEANING-CYCLE AND ECONOMIC ANALYSIS

DECLARATION

I hereby declare that the study reported in this thesis entitled above is my work and has not been submitted anywhere for any degree or other purpose. Further, I certify that the intellectual content of this thesis is the product of my work and that all the assistance received in preparing this thesis and sources have been acknowledged or cited in the reference section.

Mohammad Didarul Islam

Dept. EECE, MIST, Dhaka

EFFECT OF SOILING ON SOLAR PANELS: IN-FIELD OUTPUT
CHARACTERIZATION FOR CLEANING-CYCLE AND ECONOMIC
ANALYSIS

A Thesis

By

Mohammad Didarul Islam

DEDICATION

Dedicated to my Supervisor (Dr. M. Ryyan Khan) for supporting and
encouraging me to believe in myself

Dedicated to my parents, grandmother (Nani), and grandfather (Bhaiya) for
providing me the opportunities for my higher studies

Dedicated to my beloved wife (Romana Jahan) for supporting me in every
moment during writing this thesis paper

ABSTRACT

Effect of Soiling On Solar Panels: In-Field Output Characterization for Cleaning Cycle and Economic Analysis

Photovoltaics (PV) system is a prominent renewable energy technology that converts sunlight into electricity. This study investigates the impact of uniform and non-uniform soiling on the performance of photovoltaic (PV) panels. Soiling refers to the accumulation of dust on the surface of solar panels. This reduces the amount of sunlight reaching the solar cells and thus decreases the energy output. Uniform soiling occurs when the dust is evenly distributed on the surface, while non-uniform soiling occurs when the dust is unevenly distributed. In this thesis, we have conducted experiments and analyses using two types of mainstream PV technology (namely, monofacial and bifacial panels) to evaluate the respective effects of soiling. **For uniform soiling conditions**, we analyze the (i) tilt-dependent soiling rate and (ii) the techno-economic analysis under the soiling-cleaning cycle. Firstly, we developed an empirical soiling rate model that helped us to estimate the tilt-dependent soiling rate of that particular location. This implies the soiling rate at an arbitrary tilt can be estimated if we know the soiling rate of only one tilt angle PV panel. Secondly, we analyzed the energy output revenue of various tilt angle PV panels under uniform soiling conditions. From this analysis result, we were able to determine the optimum cleaning cycle for each tilt angle. We also conducted a techno-economic analysis based on the optimum cleaning cycle condition. Finally, at the optimum cleaning cycle, a PV panel can generate the maximum revenue. Therefore, the PV power plant should adhere to the optimum cleaning cycle to maximize its revenue. The PV power plant should follow the optimum cleaning cycle procedure to maximize its revenue. The study finds that the soiling rate is inversely proportional to the tilt angle, meaning that higher tilt angles have lower soiling rates or vice-versa. The study shows that a 30° tilt angle PV panel has maximum revenue and energy generation in Dhaka. The optimum cleaning cycle ranges from 4 to 6 days depending on the tilt angle. Furthermore, **non-uniform soiling conditions** and partial shading have been analyzed through our designed I-V scanner. This study aims to understand the effect of partial shading and non-uniform soiling on PV panels by conducting various controlled experiments. The experiments show that non-uniform soiling, such as bird droppings, significantly affects the PV panel output and can cause a drastic reduction in energy production. Therefore, immediate cleaning intervention is necessary to mitigate the effect of non-uniform soiling on PV panels. The study in this thesis is important for PV power plants to maximize their revenue by balancing the revenue and the net cleaning cost. The study enhances the understanding of soiling physics and its effect on the solar panel tilt angle for the South Asian region. The study also provides insights into the effect of uniform and non-uniform soiling on the solar panel energy output using infield characterization.

সারসংক্ষেপ

Effect of Soiling on Solar Panels: In-Field Output Characterization for Cleaning Cycle and Economic Analysis

সৌর প্যানেলের মাধ্যমে সৌরশক্তিকে বিদ্যুৎ শক্তিতে রূপান্তরিত করা যায়। এই গবেষণা ইউনিফর্ম এবং নন-ইউনিফর্ম ধূলি জমা, যা সৌর প্যানেলের উপর জমতে পারে তার প্রভাব নিয়ে আলোচনা করা হবে। সৌর প্যানেলের উপর ধূলি জমলে তার সূর্যরশ্মিকে সৌর কোষের ভিতরে পৌঁছাতে বাধা দেয় যার ফলে সৌর-প্যানেলের বিদ্যুৎ উৎপাদনের কার্যক্ষমতা হ্রাস পায়। সৌর প্যানেলের উপর যদি ধূলিকণা সবদিকে সমানভাবে জমা হয় তখন তাকে ইউনিফর্ম ধূলি জমা বলে। সৌর প্যানেলের এর উপর যদি ধূলিকণা সবদিকে সমানভাবে না জমায় তখন তাকে নন-ইউনিফর্ম ধূলি জমা বলে। এই গবেষণামূলক প্রবন্ধে বহুল প্রচলিত দুই ধরনের সৌর প্যানেল নিয়ে গবেষণা করা হয় যা মনোফেসিয়াল বাইফেসিয়াল সৌর প্যানেল নামে পরিচিত। ইউনিফর্ম ধূলি জমা অবস্থায় আমরা বিভিন্ন পরীক্ষা এবং তাদের ফলাফল বিশ্লেষণ করবো। যা কোন নির্ভর কোন নির্ভর ধূলি জমার হার এবং প্রযুক্তি অর্থনৈতিক বিশ্লেষণের জন্য ধূলি জমা এবং তা পরিষ্কার করা সংক্রান্ত বিষয়কে গুরুত্ব দেয়া হয়েছে। প্রথমত আমরা পরীক্ষামূলক একটি সূত্র সম্পাদন করেছি যা আমাদের নির্দিষ্ট অঞ্চলের যে কোন কোন স্থাপিত সৌর প্যানেলের উপর ধূলি জমার হার সম্পর্কে ধারণা দিতে পারে। দ্বিতীয়তঃ ইউনিফর্ম ধূলি জমা অবস্থায় আমরা গবেষণায় ব্যবহৃত প্রত্যেকটি কোন স্থাপিত সৌর প্যানেল কর্তৃক উৎপাদিত বিদ্যুৎ শক্তির অর্জিত আয় হিসেব করেছি। সর্বোত্তম পরিষ্কার করার চক্র কে প্রাধান্য দিয়ে আমরা প্রযুক্তি অর্থনৈতিক বিশ্লেষণ ও করেছি। অবশেষে আমরা এই সিদ্ধান্তে উপনীত হয়েছি একটি সৌর বিদ্যুৎ কেন্দ্র সর্বোত্তম পরিষ্কার চক্র অনুসরণ করে সৌর প্যানেল পরিষ্কার করলে সর্বোচ্চ আয় করতে পারবে। তাই সর্বোচ্চ আয় করার জন্য সৌর বিদ্যুৎ কেন্দ্রগুলোকে সর্বোত্তম পরিষ্কার চক্র অনুসরণ করা উচিত। আমরা এই গবেষণা থেকে জানতে পেরেছি সৌর প্যানেলের উপর ধূলি জমার হার ওই সৌর প্যানেলের স্থাপিত কোণের মানের সাথে ব্যস্তানুপাতিক। এর অর্থ হচ্ছে যদি স্থাপিত সৌর প্যানেলের কোণ বেশি হয় তাহলে সৌর প্যানেলের উপর ধূলি জমার হার কম হবে। আমাদের গবেষণা দেখিয়েছে যে ৩০ ডিগ্রি কোণে স্থাপিত সৌর প্যানেলের মাধ্যমে ঢাকা অঞ্চলের সর্বোচ্চ বিদ্যুৎ শক্তি উৎপাদন করা যায় ও অর্থ আয় করা যায়। বিভিন্ন কোণের উপর নির্ভর করে সর্বোত্তম পরিষ্কার চক্র ৪ থেকে ৬ দিন পর্যন্ত হয়ে থাকে। অধিকন্তু সৌর প্যানেলের উপর অ ইউনিফর্ম ধূলি জমা ও আংশিক ছায়া পড়ার প্রভাব কে বোঝার জন্য আমরা একটি আইভী স্ক্যানার নকশা এবং বাস্তবায়ন করেছি। এই গবেষণায় সৌর প্যানেলের উপর নন-ইউনিফর্ম ধূলি জমা ও আংশিক ছায়ার প্রভাব বোঝার জন্য আমরা কিছু নিয়ন্ত্রিত পরীক্ষা সম্পাদন করেছি। পরীক্ষালব্ধ উপাত্ত দ্বারা আমরা বুঝতে পেরেছি ইউনিফর্ম ধূলি জমা যেমন সৌর প্যানেলের উপর পাখির বিষ্ঠা পড়লে তা নাটকীয়ভাবে সৌর প্যানেলের বিদ্যুৎ উৎপাদনকে ব্যাহত করে। তাই নন-ইউনিফর্ম ধূলি জমা হলে সৌর প্যানেলকে দ্রুততার সাথে পরিষ্কার করতে হবে। এই গবেষণা হতে প্রাপ্ত উপাত্ত সৌর বিদ্যুৎ কেন্দ্রের সৌর প্যানেলগুলোর পরিষ্কার করার জন্য ব্যয় ও বিদ্যুৎ কেন্দ্র হতে অর্জিত আয়ের মধ্যে ভারসাম্য বজায় করে সৌর বিদ্যুৎ কেন্দ্রের জন্য সর্বোচ্চ আয় নিশ্চিত করতে পারবে। দক্ষিণ এশিয়ায় সৌর প্যানেলের উপর ধূলি জমার হার ও এর প্রভাব সম্পর্কে খুব ভালো ধারণা পাওয়া যাবে। এ গবেষণা হতে প্রাপ্ত উপাত্ত হতে। এই গবেষণা হতে সৌর প্যানেল ওপর ইউনিফর্ম ও নন-ইউনিফর্ম ধূলি জমার প্রভাব সম্পর্কে খুব ভালোভাবে জানা যাবে যা আসল সৌর বিদ্যুৎ কেন্দ্রের সকল বৈশিষ্ট্য বহন করে।

ACKNOWLEDGEMENTS

The author would like to express his deep gratitude to Associate Professor Dr. Mohammad Ryyan Khan, his research supervisor, for his patient guidance enthusiastic encouragement, and useful critiques of this research. Prof. Ryyan's door was always open for the author to discuss anything related to this research project. He allowed the author to work independently in this research work. He was very patient in every failed step that the author made and guided him (the author) toward a successful path. He taught the author, how to do research and also show him (the author) to be an independent thinker as well as to be a good human being. A few words are not enough to describe Prof. Ryyan's generosity. The author shows his ultimate respect for Prof. Ryyan's effort in this research work.

The author would also like to thank his Co-Supervisor Associate Professor Dr. Md Aminul Islam for his advice and assistance in keeping the author updated regarding the recent guideline needed for the research.

The author is thankful to Associate Professor Dr. Redwan Noor Sajjad for his advice and suggestions for the research work. The author acknowledges the generosity of the previous Head of the Department, Professor Dr. A K M Nazrul Islam.

The author gratefully thanks Jabir Bin Jahangir, Research Assistant of Khan SLR group for his support in developing the datalogger software for this research work. The author is also thankful to Shahadat Sarker Shakir and Mahmud Al Tamim, Research Assistant of Khan SLR group for their support and suggestions for setting up the experimental setup on the East West University rooftop.

The author would also like to extend his thanks to the officials, security guards, messengers, and all of the supporting staff of East West University, Bangladesh for allowing the author to conduct the research comfortably during the time of the pandemic.

The Author shows his profound respect and thanks to the ICT ministry of Bangladesh and East West University Center of Research and Training for funding this research work.

TABLE OF CONTENTS

| | |
|--|-----|
| ABSTRACT..... | i |
| সারসংক্ষেপ..... | ii |
| ACKNOWLEDGEMENTS..... | iii |
| TABLE OF CONTENTS..... | iv |
| LIST OF FIGURES | vii |
| LIST OF TABLES | x |
| LIST OF ABBREVIATIONS..... | xi |
| CHAPTER 1: INTRODUCTION | 1 |
| 1.1 Background of the Study..... | 1 |
| 1.2 Related Works | 2 |
| 1.3 Motivation of the Work..... | 4 |
| 1.4 Objective with Specific Aims | 6 |
| 1.5 Research Outcomes | 6 |
| 1.6 Thesis Organization..... | 7 |
| CHAPTER 2: LITERATURE REVIEW | 8 |
| 2.1 PV Panel Uniform Soiling | 8 |
| 2.2 PV Panel Non-uniform Soiling Detection Technique and Analysis..... | 10 |
| 2.3 Research Work Based on Research Gaps..... | 13 |
| CHAPTER 3: EXPERIMENTAL AND ANALYSIS METHODOLOGY | 15 |
| 3.1 Experimental Procedures..... | 15 |
| 3.1.1 Testing Site Location | 15 |
| 3.1.2 PV Panel Frame Design and Setup Layout..... | 16 |
| 3.1.3 PV Panel Arrangement and Cleaning Cycle | 16 |
| 3.2 Data Transmission Component (Data Logger)..... | 18 |
| 3.2.1 Data Transmission Technique..... | 18 |
| 3.2.2 Data Logger in PCB..... | 19 |
| 3.3 PV Module Connection..... | 20 |
| 3.3.1 Monofacial PV Panel Connection..... | 20 |
| 3.3.2 Bifacial PV Panel Connection | 21 |
| 3.4 Experimental Setup in Testing Site..... | 22 |
| 3.5 Cleaning Procedure to Mitigate the Soiling..... | 23 |

| | |
|--|----|
| 3.5.1 Manual Cleaning | 23 |
| 3.5.2 Automated Cleaning Procedure | 23 |
| 3.6 Methodology of Analysis | 24 |
| 3.6.1 Measurements and Integrated Input/output Data..... | 24 |
| 3.6.2 Performance Ratio (<i>PR</i>)..... | 24 |
| 3.6.3 Soiling Rates (<i>SR</i>)..... | 25 |
| 3.6.4 Revenue and Cleaning Cycle Calculation | 25 |
| 3.6.5 Revenue Analysis Considering Whole Year | 26 |
| CHAPTER 4: RESULT ANALYSIS AND DISCUSSION | 27 |
| 4.1 Analysis of Mono-Facial PV Panels..... | 27 |
| 4.1.1 Evaluating Soiling Rate of Monthly Clean PV Panels at Various TiltAngles ... | 27 |
| 4.1.2 Evaluating Soiling Rate of Weekly Clean PV Panels at Various Tilt Angles.... | 29 |
| 4.2 Rainfall Data during the Experiment | 30 |
| 4.3 Observing Angle Dependence of Different Tilt Angles Soiling Rate | 30 |
| 4.4 Empirical Approach of Angle Dependence of Soiling Rate | 32 |
| 4.5 Optimum Cleaning Cycle of Different Tilt Angle | 33 |
| 4.6 Energy Generation Comparison between Different Tilt Angles..... | 34 |
| 4.7 Revenue Analysis for Monofacial PV Experimental Setup..... | 35 |
| 4.8 Analysis of Bifacial PV Panels | 37 |
| 4.8.1 Evaluating Soiling Rate of Bi-Facial PV Panels at Various Tilt Angles..... | 37 |
| 4.8.2 Optimum Cleaning Cycle of Bifacial PV Panels..... | 38 |
| 4.9 Revenue Analysis for Bifacial PV Experimental Setup..... | 39 |
| CHAPTER 5: NON-UNIFORM SOILING ECONOMIC ANALYSIS..... | 41 |
| 5.1 IV Scanner Design Concept..... | 42 |
| 5.2 PV Module Connection..... | 42 |
| 5.3 I-V Scanner Circuit Diagram | 43 |
| 5.4 Experimental Methodology..... | 44 |
| 5.4.1 Experimental Data Analysis from Reading Data..... | 46 |
| 5.5 Normalized Experimental Data Analysis | 47 |
| 5.6 MPP Comparison of Experiment B, C, and D | 49 |
| 5.7 Multiple String Coverage of PV modules | 49 |
| 5.8 Correlation with Non-Uniform Soiling and Bird-dropping | 50 |
| 5.9 Economic Analysis of Non-uniform Soiling..... | 51 |
| 5.10 Revenue Analysis for Non-uniform Soiling..... | 52 |

| | |
|---|----|
| CHAPTER 6: CONCLUSIONS | 55 |
| 6.1 Monofacial PV Setup Experiment | 55 |
| 6.2 Bifacial PV Setup Experiment | 55 |
| 6.3 Non-uniform soiling and Economic Analysis | 56 |
| 6.3.1 Designing I-V Scanner and Conducting Experiment..... | 56 |
| 6.4 Summary of Techno-Economic Analysis under Uniform Soiling Conditions | 57 |
| 6.5 Summary of Techno-Economic Analysis under Non-uniform Soiling Conditions | 57 |
| 6.6 Implications of this Thesis | 58 |
| 6.7 Limitations of the Research Work | 59 |
| 6.8 Future Work of the Research | 59 |
| REFERENCES... .. | 60 |
| LIST OF PUBLICATIONS | 66 |

LIST OF FIGURES

| | |
|--|----|
| Fig. 1.1 Global Maps of (a) GHI [4], and, (b) Soiling rate (%/day) [4]–[7]..... | 2 |
| Fig. 2.1 Soiling rate measurement using the Fixed Rate Precipitation method [32]. | 9 |
| Fig. 2.2 Revenue loss in (\$ billion) due to soiling solar panels globally. | 10 |
| Fig. 2.3 Non-uniform soiling on (a) bottom edge, (b) dew drop, (c) due to bird-dropping [36]. | 10 |
| Fig. 2.4 Effects of (a) uniform soiling, (b) non-uniform soiling, and (c) partial shadings [8]. | 12 |
| Fig. 3.1 Areal view of the testing site (a) top view, (b) side view. | 15 |
| Fig. 3.2 PV module adjustable frame design front view (Monofacial Setup)..... | 16 |
| Fig. 3.3 PV module adjustable frame design front view (Bi facial Setup). | 16 |
| Fig. 3.4 Monofacial PV panel experimental setup layout (a) top view, (b) side view..... | 17 |
| Fig. 3.5 Bi-facial PV panel experimental setup layout (a) top view, (b) side view. | 18 |
| Fig. 3.6 Data Acquisition through Cloud Server. | 19 |
| Fig. 3.7 Datalogger (a) PCB design setup, (b) Load circuit, and (c) Datalogger in house setup. | 19 |
| Fig. 3.8 PV Modules Connection for monofacial PV panel Experimental Setup..... | 20 |
| Fig. 3.9 PV Modules Connection for bifacial PV panel Experimental Setup..... | 21 |
| Fig. 3.10 Experimental setup of mono-facial PV panels. | 22 |
| Fig. 3.11 Experimental setup of, (a) bi-facial PV panels, (b) bifacial PV modules..... | 22 |
| Fig. 4.1 Soiling rates, cleaning cycles and rainfall of mono-facial monthly clean PV panels | 28 |
| Fig. 4.2 Soiling rates, cleaning cycles and rainfall of mono-facial weekly clean PV panels | 29 |
| Fig. 4.3 Rainfall Data of January to March 2022..... | 30 |
| Fig. 4.4 Angle dependence of PV panels soiling rates of monthly and weekly cleaned panel. | 31 |
| Fig. 4.5 Angle dependence of PV panels relationship with soiling rate by empirical approach | 32 |
| Fig. 4.6 Relationship between revenue and cleaning cycle of tilt angles monofacial PV panel | 34 |
| Fig. 4.7 Energy generation of PV panel in different tilt angles | 35 |
| Fig. 4.8 Revenue comparison of soiling less, daily, weekly and monthly cleaned panel.. | 36 |

| | |
|--|----|
| Fig. 4.9 Soiling rates between cleaning cycles and rainfall (a) 0-degree tilt angle, (b) 20-degree tilt angle, and (c) 30-degree tilt angle..... | 37 |
| Fig. 4.10 Relationship between revenue and cleaning cycle, (a) 0-degree tilt angle, (b) 20-degree tilt angle, and (c) 30-degree tilt angle..... | 38 |
| Fig. 4.11 Revenue comparison of uncleaned and optimally cleaned panel | 40 |
| Fig. 5.1: I-V curve of MOSFET and PV module and I-V curves intersecting point | 42 |
| Fig. 5.2 (a) Connection of PV modules, (b) bypass diode connection in PV modules..... | 43 |
| Fig. 5.3. I-V scanner schematic circuit diagram | 43 |
| Fig. 5.4: (a) Individual solar cell cover (%) variation have been defined here. Various experiment conditions are shown: (b) experiment B: solar cell cover (%) variations in string 1, (c) experiment C: string1 fixed 25% cover, string2 individual cell cover (%) variations, (d) experiment D: string1 fixed 25% cover, string1 another cell cover (%) variations. (e) Experimental setup of I-V scanner. (f) Example of the conducted experiment, i.e. expC4 of table-II..... | 45 |
| Fig. 5.5. (a) I-V curve of experiment A (a cell of string1, 25% cover; another cell of string 1, 25% cover), (b) P-V curve of experiment A, (c) I-V curve of experiment B (string 1 cell 0%, 25%, 50%, 75% and 100% cover variation), (d) P-V curve of experiment B, (e) I-V curve of experiment C (string 1, a cell 25% fixed cover, string 2 another randomly picked cell, 0%, 25%, 50%, 75%,and 100% cover variation), (f) P-V curve of experiment C, (g)) I-V curve of experiment D (string 1, a cell 25% fixed cover, string 1 another randomly picked cell, 0%, 25%, 50%, 75%, and 100% cover), (h) P-V curve of experiment D..... | 46 |
| Fig. 5.6. (a) Normalized I-V curve of experiment A (a cell of string1, 25% cover; another cell of string 1, 25% cover), (b) Normalized P-V curve of experiment A, (c) Normalized I-V curve of experiment B (string 1 cell 0%, 25%, 50%, 75% and 100% cover variation), (d) Normalized P-V curve of experiment B, (e) Normalized I-V curve of experiment C (string 1, a cell 25% fixed cover, string 2 another randomly picked cell, 0%, 25%, 50%, 75% and 100% cover variation), (f) Normalized P-V curve of experiment C, (g) Normalized I-V curve of experiment D (string 1, a cell 25% fixed cover, string 1 another randomly picked cell, 0%, 25%, 50%, 75% and 100% cover variation), (h) Normalized P-V curve of experiment D..... | 48 |
| Fig. 5.7. Maximum Power Point comparison of experiment B, C, and D. | 49 |
| Fig. 5.8: Experiment E (a) normalized I-V curve, (b) normalized P-V curve. | 50 |

Fig. 5.9.: Soiling band schematic diagram (a) triangular, (b) rectangular, (c) transverse trapezoidal, (d) bird-dropping schematic diagram on PV panel..... 51

Fig. 5.10. Performance ratio versus cleaning cycle (a) without non-uniform soiling, (b) with non-uniform soiling conditions (edge soiling due to machine or manual cleaning), and (c) with non-uniform soiling conditions (bird-droppings, snowfall, sand storm)... ..52

Fig. 5.11. Relationship between (a) normalized revenue and decreasing factor of performance ratio (γ) (b) normalized revenue and covered area (%) due to non-uniform soiling..... .53

Fig. 5.12. Relationship between (a) revenue and decreasing factor of performance ratio (γ) (b) revenue and covered area (%) due to non-uniform soiling.....54

LIST OF TABLES

| | |
|---|----|
| Table 3.1 Electrical Parameter for Monofacial PV Panel Specification..... | 21 |
| Table 3.2 Electrical Parameter for Bifacial PV Panel Specification..... | 21 |
| Table 4.1 Monthly Cleaned Panel Soiling Rate (%)..... | 28 |
| Table 4.2 Weekly Cleaned Panel Soiling Rate (%)..... | 29 |
| Table 4.3 Techno-Economic Analysis Summary of Monofacial PV setup..... | 33 |
| Table 4.4 Techno-Economic Analysis Summary of Bifacial PV setup..... | 39 |
| Table 5.1: Electrical Parameters of PV Module Specifications..... | 43 |
| Table 5.2 Description of the Conducted Partial Shading Experiment..... | 44 |

LIST OF ABBREVIATIONS

| | |
|--------------|---|
| β | Tilt Angle |
| C | Cleaning Cost |
| DC | Daily Cleaned |
| I_{sc} | Short Circuit Current |
| I | Current |
| MC | Monthly Clean |
| MPP | Maximum Power Point |
| $MOSFET$ | Metal Oxide Silicon Field Effect Transistor |
| PL | Performance Loss Factor |
| PR | Performance Ratio |
| $PV\ Module$ | Photovoltaic Module |
| R | Tariff Rate |
| SL | Soiling Less Panel |
| SR | Soiling Rate |
| T_c | Cleaning Cycle |
| UC | Unclean |
| V | Voltage |
| WC | Weekly Clean |

CHAPTER 1

INTRODUCTION

1.1 Background of the Study

Photovoltaics (PV) modules are devices that convert sunlight energy into electrical energy. Photovoltaic power is becoming more popular today because of its reasonable price and easy installation. PV panels are also becoming more affordable every year, which is another reason for their rapid growth. Electricity generation from PV panels is very important for mankind to transition from conventional energy sources to green energy sources.

The PV capacity increased from 483.1 GW in 2018 to 580.2 GW in 2019, a 21% growth. According to the International Energy Agency (IEA), the global PV energy output rose by 773 GW in 2021 compared to 2019, which means a proportional growth (%) of PV capacity of nearly 25% [1]–[3]. The adoption of PV farms is increasing rapidly on a global scale. Asia leads the PV production, with China, Japan, and India having PV capacities of 175 GW, 55.5 GW, and 28.6 GW respectively. Europe is the second-largest region for PV installation, with Germany having 45.9 GW, Italy having 20.12 GW and the UK has 13.4 GW of PV capacity [1].

PV modules use solar cells to convert sunlight into electricity. The amount of sunlight that reaches the PV module affects its electricity generation. If anything blocks the sunlight (such as bird droppings or dirt), the PV panel's energy production will decrease significantly. Over time, the dirt will accumulate on the PV panel surface. The accumulated dirt prevents the sunlight from reaching the solar cells, which reduces the PV panel's electricity output. The soiling loss of PV panels refers to the decrease in electricity generation caused by the dirt on the panels.

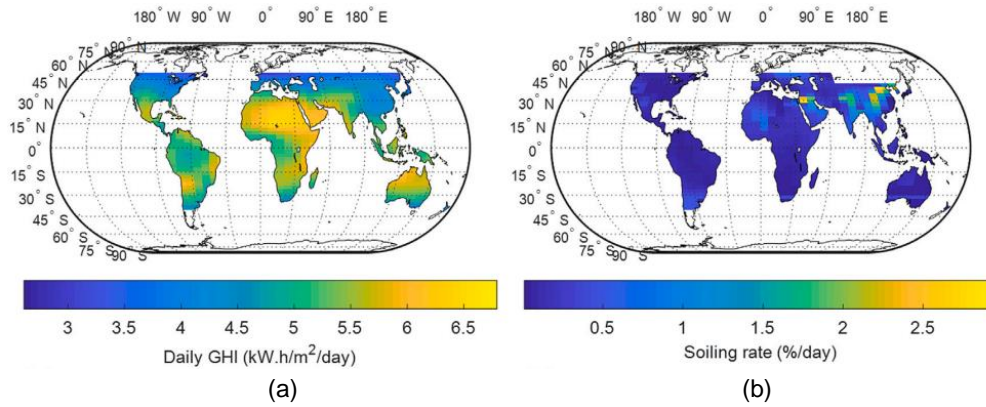


Fig. 1.1 Global Maps of (a) GHI [4], and, (b) Soiling rate (%/day) [4]–[7]

Fig-1.1 shows the global maps of Global Horizontal Irradiance (GHI) and also the soiling rate. Global Horizontal Irradiance is measure the amount of sunlight received by the surface. High GHI areas have high soiling rates, which increase the soiling loss and reduce the performance and revenue of the PV power plants. Therefore, mitigating soiling loss is a major challenge for maintaining maximum revenue in these areas.

1.2 Related Works

The global electricity demand for domestic and industrial purposes has increased due to the rapid industrialization of the modern world. Various countries plan to add 327.6 GW of renewable energy to the world's electricity generation by 2025, with solar energy being the main source among other renewables [8], [9]. Different environmental parameters (such as soiling, humidity, and temperature) can affect the electricity generation of PV panels. Engineers need to consider these factors to maximize the revenue from the PV power plant.

Soiling loss is one of the main elements that greatly reduces PV performance, but it is sometimes overlooked. Soiling loss is different according to the specific location and sites. Therefore, the individual site must need to conduct assessments for determining the soiling rate accurately [9]. Soiling on surfaces can either be uniform or non-uniform. Uniform soiling loss is the process where dust accumulates on the PV module surface naturally with time. This, accumulation of dust absorbs, reflects, and resists direct sunlight to enter the PV module PV cell. By this, the electricity generation of the PV module decreases significantly. If soiling increases, the power generation will be decreased [10]. The optimal cleaning cycle

can ensure maximum revenue in PV power plants [8]. The optimum cleaning cycle makes a balance between revenue and cleaning costs in order to maximize revenue for a PV farm. Soiling rates vary by location and time of year [11]. The tilt angles of PV modules and the soil band structure also affect the soiling loss rates of PV modules [12], [13]. For instance, while the Middle East and North America (MENA) locations have good insolation, they are also highly soil-prone, therefore the cleaning cycle should be 5 to 6 days for maximum revenue [4].

The majority of earlier research in the literature has taken the uniform soiling impact on the PV module into account. Most of the prior studies in the literature have been done considering the uniform soiling effect on the PV module. Different shadowing on PV cells results from irregular soiling conditions. It causes various shades to appear on PV cells. Non-uniform soiling (e.g., accumulated edge dust or snow, bird droppings) partially shades panel cells, causing power loss, hotspots, and even solar cell breakdown in PV panels [14], [15]. Hot spots led to a temperature difference of nearly 20°C between the soiled and non-soiled PV modules [8]. Non-uniform soiling takes different types of shapes on the edge of the PV module [13]. PV panels can suffer power loss, hotspots, and even solar cell breakage due to uneven soiling (e.g., accumulated edge dust or snow, bird droppings). Researchers discovered irregular soiling on the PV module's right corner, which covered 0.5% of the surface and resulted in a 9% power drop [8]. Due to the non-uniform soiling condition described in the literature study, PV plant power output can be decreased by up to 10% [16]–[19]. A 2 MW system in Southern Spain likewise showed non-uniform losses in current and power [17]. To comprehend the non-uniform soiling impact, it is necessary to examine variations in the I-V and P-V properties of the photovoltaic panel [20], [21].

Previous research on partial shadowing suggests that if a single PV module cell is partially shaded by soil, the PV module's ability to generate power may suffer. The output of several PV modules can substantially decrease if they get un-uniformly soiled, and electricity generation cannot be sustained without a cleaning intervention [15]–[19].

In Bangladesh, the summer and winter months are both quite vulnerable to soiling. However, the wet season brings about a lot of rain, which also has an impact on PV generation. The combination of these circumstances has not received enough research attention in the literature. After studying the prior literature, we have realized that to understand the soiling

effect on the PV module for the Bangladesh region, we must do an extensive study because the soiling rate in this South Asian region fluctuates with the season. To optimize economic income while balancing cleaning costs, economic analysis of Bangladesh's PV generation should consider uniform and non-uniform soiling. Cleaning correctly might result in a 4.5% increase in income as opposed to cleaning every month [4].

1.3 Motivation of the Work

Solar energy is becoming more popular day by day in Bangladesh. People in rural areas have installed off-grid PV systems on their rooftops. On the other hand, the government and different private organizations have come forward to invest in solar power plant projects. Bangladesh has a total of 356.01 MW of off-grid PV energy and 321.41 MW of on-grid PV energy. The largest PV plant in Bangladesh is located in Mongla Upazila, Bagerhat, with a capacity of 100 MW. It is operated by the Bangladesh Power Development Board (BPDB) [22]. Moreover, many private and government agencies are planning to install more PV power plants in the next year, which will reduce the dependence on fossil fuels for electricity generation.

The installed power generation capacity of Bangladesh is now over 24,000 MW, supported by 146 power plants, captive sources, and off-grid sources. Only 776 MW of it, or around 3% of the total amount of power produced, comes from renewable sources. In the future, the contribution of renewable energy will be increased significantly. In the future, the Bangladesh government has a goal of generating more than 4100 MW of electricity from renewable energy sources by 2030. 2,277 MW of the energy will come from solar power, followed by 1,000 MW from hydropower and 597 MW from wind [23]. In the future renewable energy will play a vital role in Bangladesh's power sector and solar energy will be there as a key factor. The main obstacle to implementing the solar power plant is that it takes too much land. Therefore, the locations of these solar power plants will be scattered. Some of the lands may also become infertile or prone to soiling, which makes the PV power plants in these areas more susceptible to soiling for the PV panels

In Dhaka, Bangladesh, researchers have found that the soiling rate of 0° , 24° , and 90° tilted panels was 0.0157/day, 0.0078/day, and 0.00081/day, respectively [11]. In this condition, researchers discovered that a monofacial farm that is cleaned once a month for the described tilted panel might lose more than 10% of its assessed revenue [9]. Soiling loss reduces the power generation of PV power plants. As a result, the PV power plant earns less revenue. Cleaning the PV power plant three times a month at a specific location can increase the system performance by 12% [24].

Cleaning PV farms requires water, an essential natural resource. According to a journal article in *Renewable and Sustainable Energy Reviews*, PV panels use between 0.5 and 20 liters of water per square meter for cleaning. MIT researchers estimate that 10 billion gallons of water are used annually for this purpose, which could supply up to 2 million people with water [25]. Bangladesh faces a serious water shortage due to its high population density and low natural resources. A World Resources Institute report classifies Bangladesh as a country with high water stress, meaning that water demand sometimes exceeds supply throughout the year. Most of the photovoltaic fields in Bangladesh are located in rural areas outside of Dhaka. Using too much water for cleaning could cause water scarcity in these areas, which would affect their agriculture sector. Therefore, finding an optimal cleaning method for PV fields is important for the Bangladesh region because it will minimize the usage of water for the frequent cleaning.

Bangladesh has a lot of soil in the summer and winter seasons, which affects PV generation. The rainy season also has a negative impact on PV generation. The literature lacks studies on these scenarios. Most of the previous studies have assumed uniform soiling on the PV panel. However, non-uniform soiling (such as edge dust, bird droppings, or snow) can partially shade the panel cells, causing power loss, hotspots, and even solar cell damage. Previous studies on partial shading show that even a small amount of soil on a single PV cell can reduce the PV module's power generation. If several PV modules are non-uniformly soiled, the output can drop significantly until they are cleaned. Therefore, this work also aims to understand the effect of non-uniform soiling on PV module performance. Partial shading and non-uniform soiling have similar effects [6].

The literature review reveals that the soiling rate in this South Asian region varies with the seasons. Therefore, we need more research on the location-specific effects of soiling on the

PV module in Bangladesh. We also need to conduct a techno-economic analysis of PV generation in Bangladesh, considering both uniform and non-uniform soiling. This will help us optimize the revenue by balancing the cleaning costs. To maximize the power output from the solar power plant, we should investigate all the natural and unnatural factors that affect solar panels in Bangladesh.

1.4 Objective with Specific Aims

The objective of the research is the following-

- i. To evaluate the soiling rate of bi-facial and mono-facial PV panels at various tilt angles.
- ii. To observe variations in PV panel I-V characteristics as a result of non-uniform soiling.
- iii. To assess the angle dependency of soiling rate concerning PV panel's tilt angles and determine the relationship between them through an empirical approach
- iv. To perform an economic analysis to evaluate losses, costs, and revenue at various cleaning intervals, considering uniform and non-uniform soiling rates.

1.5 Research Outcomes

This thesis examines how soiling affects PV panels with different tilt and weather conditions, especially in Bangladesh. It shows how uniform and non-uniform soiling on panels can reduce the yield significantly. It also evaluates the economic impact of a PV power plant under different soiling conditions. Moreover, it observes how the soiling rates vary with the tilt angle of the PV modules in South Asian region. This work also propose a formula to estimate the soiling rate for any tilt angle by using an empirical approach, based on the soiling rates measured for different tilt angles of PV panels in the testing site (South Asia region).

This study designed and implemented an I-V scanner to investigate the effect of non-uniform soiling and partial shading effect on solar panel. It also performed various

controlled experiments to measure the effect of non-uniform soiling and partial shading effect. It analyzes how non-uniform soiling can greatly reduce the revenue of a PV power plant. It also studies how to optimize the revenue by choosing the optimum cleaning cycle that balances the electricity sold and the net cleaning cost.

1.6 Thesis Organization

This thesis is organized as follows: Chapter 1 introduces the background and motivation of this study, as well as the objectives and expected outcomes. Chapter 2 reviews the recent research on uniform soiling scenarios in monofacial and bifacial PV farms and the effects and assessment methods of non-uniform soiling. Chapter 3 describes the experimental approach, the tools and the numerical analysis model used in this project. It also explains the data collection methods used during the experiment. Chapter 4 shows the effects of uniform soiling on monofacial and bifacial PV setups. It also shows the techno-economic analysis, the optimal cleaning cycle, the angle dependence of the soiling rate, and the empirical method. Chapter 5 discusses the design and implementation of the I-V scanner, which was used to measure the changes in PV panel I-V curves due to non-uniform soiling. It also reports the experiments done to study the effects of partial shading and non-uniform soiling on PV panel performance. Based on these experiments, chapter 5 also provides an economic analysis of non-uniform soiling on PV farm production. Chapter 6 summarizes the main findings and suggests some future work for this field of study. Chapter 7 lists the references used for the data and literature review.

CHAPTER 2

LITERATURE REVIEW

In the previous chapter, we discussed the rationale and outcomes of this research activity. We have learned how important it is to analyze the effects of soiling for specific locations. The main reason for assessing the soiling of each location is that the soiling rates vary depending on the environmental parameters. Uniform soiling is a natural phenomenon that PV farms have to deal with. Non-uniform soiling can occur at any time during the cleaning process or in a few natural conditions such as bird-dropping, strong directional wind, etc. This situation can significantly reduce the power generation of PV farms.

This chapter will review some of the major and specific contemporary research on soiling loss analysis and its effect on solar panels to understand the current state of the art.

2.1 PV Panel Uniform Soiling

Solar energy is a prominent source of renewable energy. While monofacial photovoltaic (PV) panels have been the dominant choice, bifacial PV technology is gaining industry interest due to improved manufacturing and higher yield. According to ITRPV, bifacial PV technology is expected to reach 35% of the market share by 2027 [26]. Bifacial panels collect light from both faces, thereby enhancing the bifacial PV farm output by 10-30% over monofacial farms [27]. The gain depends on the farm design variables - tilt, fixture height, spacing, etc. [27], [28], soiling loss is a natural phenomenon that reduces the output of solar panels over time. It is caused by dust deposition or dirt on the panel surface. The panel performance can be restored by cleaning interventions such as rain or manual cleaning. However, cleaning PV panels daily would increase the operational cost and reduce the profit. Therefore, the cleaning cycle should be optimized to maximize revenue.

The soiling rates of panels vary depending on the location and season. More than half of the global PV capacity is located in Southeast Asia, Europe, North America, the Middle East, and North Africa (MENA) regions [29], [30]. These regions within the sunbelt are more efficient for PV electricity generation but also more dust-prone due to higher soiling losses [31]. For example, the MENA regions have high solar radiation but also high soiling rates (SR, a) of 0.5-1%/day. This means that the panels need to be cleaned every 5 to 6 days [4] for maximized revenue. Soiling is more severe in the summer and winter seasons in South

Asia. However, the panels are naturally cleaned by the heavy and frequent rains in the wet season. The panel configuration also affects the soiling rates [11], [12].

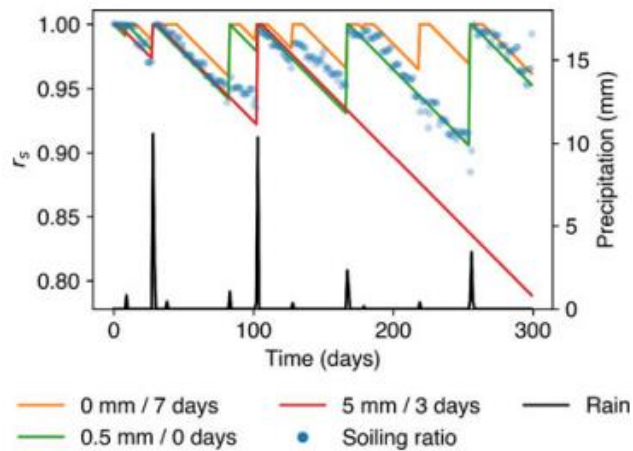


Fig. 2.1 Soiling rate measurement using the Fixed Rate Precipitation method [32].

Figure 2.1 shows how the Fixed Rate Precipitation (FRP) method is used to measure the soiling rate of PV panels. In this experiment, the researchers calculate the soiling rate by finding the slope of the performance index profile during the longest dry period. They assume that rainfall events clean the PV panels, so they choose a threshold rainfall amount that indicates effective cleaning. This rainfall threshold amount is called ‘effective rainfall’.

Most studies on soiling have focused on monofacial panels, but there are few works on bifacial panels. Bifacial PV panels can capture direct, diffuse, and ground-reflected light, and they can be installed in different configurations (tilted or vertical). Higher panel tilts usually reduce soiling [33], [34] (albeit at the cost of lowered light collection). Where there is a higher possibility of soiling loss and a limited chance to clean the panel, vertical bifacial installation may be a natural choice [11]. This is however an unwanted scenario—typically we would tilt the panels optimally for maximum output and revenue [27]. A tilted bifacial panel has different dust accumulation on the front and rear faces. Experiments in Santiago, Chile show that the soiling rates on the rear face maybe 10 times lower than on the front face [35]. Therefore, the cleaning cycle optimization should be done separately for the front and back surfaces of a bifacial panel.

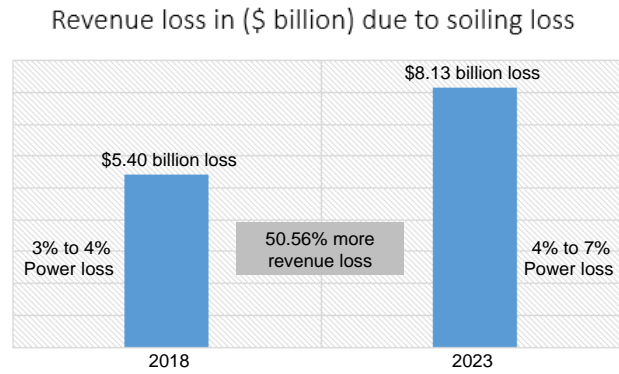


Fig. 2.2 Revenue loss in (\$ billion) due to soiling solar panel globally.

A 2018 report by PV magazine estimated that global power loss due to soiling on solar panels was between 3% and 4%, costing about \$ 5.40 billion. The researchers projected that by 2023, the power loss would increase to 4% to 7%, costing about \$ 8.13 billion [35], [36]. This means that the revenue loss would grow by almost 51% from 2018 to 2023, as shown in fig. 2.2. The revenue loss is expected to rise further in the future as the PV capacity expands worldwide.

2.2 PV Panel Non-uniform Soiling Detection Technique and Analysis

The amount of sunlight that passes through the surface of a solar panel affects how much electricity it can produce using PV modules. If anything blocks the sunlight, such as bird droppings or uneven soiling, the power generation efficiency of the PV modules goes down. The I-V (current vs. voltage) characteristics curve of a PV module shows how well it can convert solar energy. The P-V (power vs. voltage) characteristics curve of a PV module helps to find the maximum power point (MPP). Factors like partial shading, uneven soiling, and bird droppings change the I-V characteristics curve of a PV module. These effects can be analyzed by measuring the changes in the I-V curve with an I-V scanner. However, I-V scanners are not widely used in the industry because they are very expensive [21].

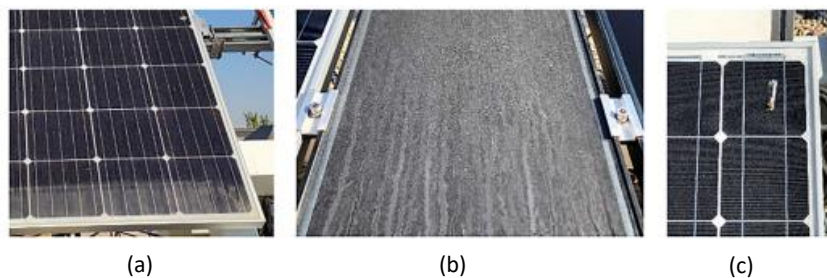


Fig. 2.3 Non-uniform soiling on (a) bottom edge, (b) solar panel after dew drop, (c) due to bird-dropping [36].

Sometimes, the soiling on the solar panels is not evenly distributed. For example, after cleaning the PV modules, some soil may remain on the bottom edge. Also, bird droppings or fog may cause patches of soiling on the panel surface, as shown in fig.2.3. Solar cells of a PV module are connected in a series consisting of multiple strings. If the bottom solar cell of any string is covered by the non-uniformly accumulated soil, then it will affect the power generation efficiency of the PV module. The studies show that the effect of non-uniform soiling on the PV module is more significant than the effect of uniform soiling [10], [37], [38]. Soiling usually builds up at the bottom or sometimes at the top of the PV module, depending on the direction of wind and rain water [17], [39]. Soiling accumulation at the bottom of PV module covers the surface of the solar cells, the free space of the bottom edge and frame, which significantly reduces the PV module performance [17]. PV modules with lower tilt angles are more prone to the soiling accumulation at its bottom edge [19], [38]. Due to the gravity force, the cleaning water are usually not enough to move these dust particles and these particles tend to accumulate steadily at the bottom edge of the PV module in different shapes [13]. Portrait or landscape configurations are generally followed to install the PV module [40]. From the studies, rectangular, triangular and transverse trapezoidal types of band shapes of accumulated soiling are observed at the bottom edge of PV module [13]. Partial shading and soiling bands that are created at the bottom edge of the PV module reduces the transmittance of incoming sunlight into the solar cells, that leads to a hotspot [41]. This localized overheated hotspot of the PV module also caused by accumulation of soiling and bird-droppings [42]. Besides, the entire area that is covered by the non-uniformly distributed accumulated soiling and bird-droppings also showed the high temperature during the field investigation [13]. These hotspots of the panel may lead to permanent damage of the PV module. The fixed area that is covered by the accumulated soiling compared to the non-soiling area may stores some water during the time of cleaning or raining for a long time on the module surface, that can damage the seal of the PV module which reduces the service life of the PV panel [43]. Now a days, solar power generation builders are designing the solar power plant without considering the effect of environmental factors and power loss of PV module due to the mismatch of the interconnected solar cells of PV module which is the result of the partial shading [44], [45]. For minimizing the mismatching of the interconnected solar cell bypass diode is used in the PV module. For 72 cells PV module, each 24 solar cell of that module contains 1 bypass diode [46]. There has been immense research on PV module under the shading conditions [47]. The temperature of the hotspot is definitely connected to non-uniform soiling, soil band structure, and non-

uniform soiling [48]. The collection of dust at the bottom corners of PV modules can cause a significant loss in performance [49].

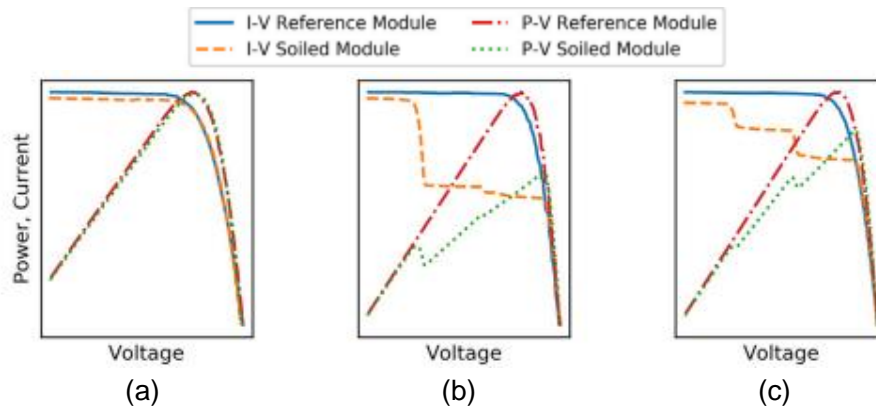


Fig. 2.4 Effects of (a) uniform soiling, (b) non-uniform soiling, and (c) partial shadings on solar panel [8]. Two Si solar panels installed on the roof of the University of Jaen in southern Spain are shown in Fig. 2.4 as an illustration of the impacts of uniform and non-uniform soiling. I-V and P-V curves of two solar panels under uniform soiling circumstances are shown in Fig.2.4 (a). Both PV modules' I-V and P-V curves have the same form under uniform soiling conditions. However, the uncleaned PV module's short circuit current is lower than the clean PV module's. Due to the consistent soiling state on the uncleaned PV module, there is a corresponding fall in the maximum power point. The soiled I-V and P-V curves exhibit a step in the maximum power under non-uniform soiling conditions, as seen in Fig. 2.4 (b). This is because the shaded cell is activated by the bypass diode. A more complex situation might result in even more than one knee in the I-V and P-V curves when partial shade occurs as a result of bird droppings on multiple sub-strings, as seen in Fig. 2.4(c).

If 0.5% of the area on the bottom edge of the panel is covered by soiling, the output of a PV panel can decrease by 9% [50]. Due to the non-uniform soiling in PV panels, power losses become 10% greater than short-circuit current losses [19]. Researchers conducted an experiment in a 2 MW PV plant in southeast Spain and found that non-uniform soiling had a greater impact on the PV panel than uniform soiling [17]. I-V scanner is an expensive device. Therefore, research on the effect of partial shading, non-uniform soiling, and bird-dropping yet is insufficient.

2.3 Research Work Based on Research Gaps

Previous studies have examined the effects of soiling and the economic benefits of optimizing the cleaning cycle for monofacial panels. To analyze how soiling affects a bifacial panel depending on its tilt, it is necessary to measure the soiling rate and use a model for the cleaning cycle analysis.

- i. In this study, we measured the output of both monofacial and bifacial panels that were clean and unclean at different tilt angles and compared their performance ratio to determine the soiling rates in Dhaka, Bangladesh, a South Asian city.
- ii. We developed a model to estimate the revenue depending on the cleaning cycle. We used the output of the clean panels and the soiling rates from our experiment to predict the revenue for different cleaning cycles for monofacial panels at 0° , 10° , 20° , 30° , 60° and 90° tilts and for bifacial panels at 0° , 20° and 30° .
- iii. This study presents a simple IV scanner that can measure the changes in the I-V characteristics curve of a PV module under real operating conditions. The designed IV scanner is relatively cheaper, simpler, and more effective than other devices. All the components of this IV scanner are commercially available, which makes it convenient, economical, and efficient for industrial use.
- iv. The aim of this experiment is to study the effect of partial or non-uniform shading on PV modules due to soiling at the bottom edge of PV modules or bird droppings. This is a controlled experiment where different solar cells are randomly selected and covered with different percentages of their area to measure the effect of shading on the I-V and P-V curves of the solar panel. The experimental results are explained in detail and the relationship between the power generated by the PV module and the percentage of coverage area is also shown.
- v. The study of this thesis discusses how the power generated by PV modules is affected by the percentage of shade covering the area, as well as the conditions of soiling and bird droppings. This kind of partial shade is different from the more

common row-to-row shading, and it should be carefully managed to avoid sub-optimal solar farm operations. However, there seems to be a lack of research on how partial shade caused by non-uniform soiling and bird droppings affects the efficiency of PV module power generation. Non-uniform soiling can severely reduce the output of PV modules. It can also significantly lower the revenue of PV power plants. Even if the PV panels are cleaned regularly, the power generation may not increase due to uneven soiling.

- vi. In this study, we conducted various selective controlled experiments. Then we evaluated the techno-economic analysis of the effect of non-uniform soiling on different cleaning cycles. We also addressed the economic analysis of the performance ratio reduction factor of the PV panel at the end of this study.

CHAPTER 3

EXPERIMENTAL AND ANALYSIS METHODOLOGY

This chapter describes the experimental setup we used to measure the soiling rates of PV panels with different tilt angles. We compared the soiling rates of monofacial and bifacial PV panels. We used a data logger that we developed in-house to save the data in a cloud server every 2 minutes. The experiment lasted for 4 months (December to March) in 2022. At the end of this chapter, we will present the methodology and the equations that we used for numerical analysis. We will also propose an equation to calculate the revenue for bifacial PV panels. This chapter builds on the previous chapter, where we discussed the economic analysis of PV fields with uniform and non-uniform soiling. We also reviewed the previous work on measuring the soiling analysis on PV panels with different tilt angles in Chapter 2.

3.1 Experimental Procedures

3.1.1 Testing Site Location

We chose to conduct our research on the East West University, Bangladesh, a multi-storied building in Dhaka city on top of the 8th floor. Before choosing this site, various shadowing effects that may affect the experiment were carefully evaluated.



Fig. 3.1 Areal view of testing site (a) top view, (b) side view.

Fig. 3.1(a), and (b) shows the top view of the testing site, the yellow side view indicating the experimental setup of the testing site for both bi-facial and mono-facial PV panels.

3.1.2 PV Panel Frame Design and Setup Layout

For this study, we must design the PV panel frame according to our specifications, with various tilt angles. There will be three (3) PV modules for each angle in the frame, which will be cleaned daily, weekly, and monthly, accordingly.

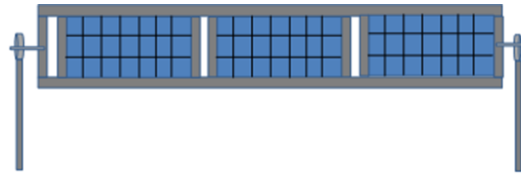


Fig. 3.2 PV module adjustable frame design front view (Monofacial Setup).

The frame has the flexibility that we can change the tilt angle of each frame according to our requirements. The mechanical design is very unique and reliable. The frame design is seen in Fig.3.2, above. Fig-3.3 represents the mechanical design of the bi-facial PV panel experimental setup.

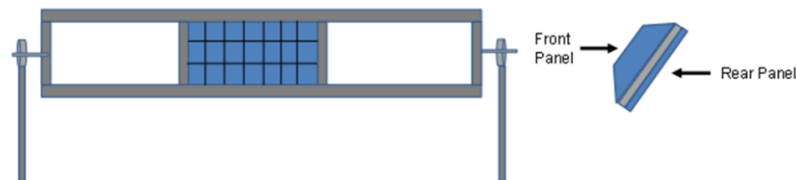


Fig. 3.3 PV module adjustable frame design front view (Bi facial Setup).

The dimension of both frames is 7' x 3'. For the bi-facial PV panel experiment, we have used two back-to-back panels to mimic a bifacial panel—this way, we could assess the output of each of the faces.

3.1.3 PV Panel Arrangement and Cleaning Cycle

Fig.3.4 illustrates the experimental setup layout of the mono-facial PV panel experimental setup top view and side view respectively. In this study, we analyzed six distinct tilt PV panels (i.e., (6 angles) \times (3 cleaning cycles) = 18 panels) for mono-facial PV soiling experimental setup: 0°, 10°, 20°, 30°, 60°, and 90°. We picked six tilt angles for the mono-facial PV soiling experimental setup to better understand the soiling mechanics on the PV module surface. We have chosen two cleaning cycles for the mono-facial PV panel experimental setup. Cleaning cycle 1 which is denoted as C1, where the PV panel was cleaned weekly, these PV panels we indicated as weekly cleaned panel or WC panel. Cleaning cycle 2 which is represented as C2, where the PV panel was cleaned monthly, these PV panels we indicated as monthly cleaned panel or MC panel.

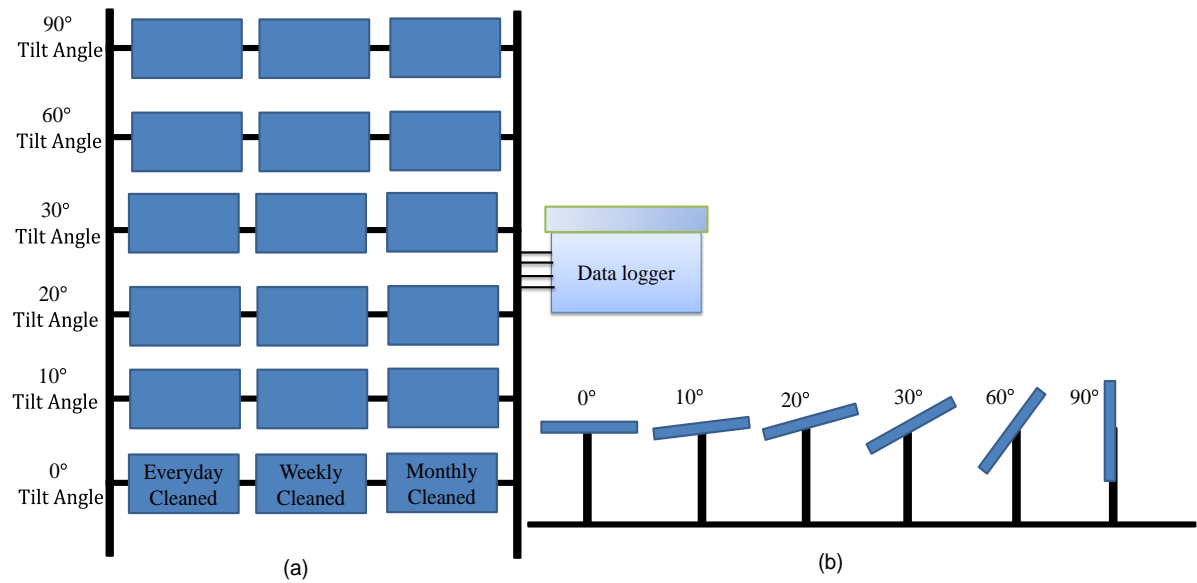


Fig. 3.4 Monofacial PV panel experimental setup layout (a) top view, (b) side view.

Fig.3.5 illustrates the experimental setup layout of the bi-facial PV panel experimental setup top view and side view consecutively. For the bi-facial PV panel experimental setup we used three different tilts. For the bi-facial PV soiling experiment: 0°, 20°, and 30° (12 panels) are chosen. In South Asia, bi-facial panels are typically set at 20° to 30°. We additionally chose 0° for the bi-facial PV module to better understand soiling effects, which will aid us in future studies. For this experiment, we have chosen an irregular cleaning cycle where the soiled bi-facial PV panel front and rear sides were cleaned randomly. Reference PV panels for both experimental setups had been cleaned very carefully using soft clothing material. During the cleaning process, only water was used to clean the heavily soiled panel. The time of cleaning the reference panel was 9.00 am. The reference panel in the thesis is denoted as the everyday cleaned panel or daily cleaned panel.

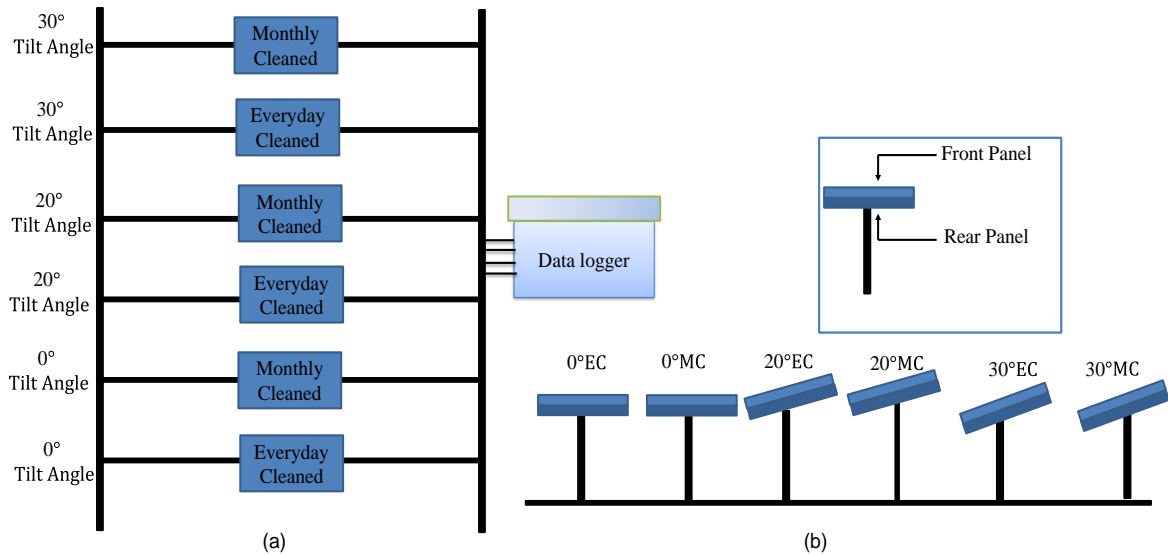


Fig. 3.5 Bi-facial PV panel experimental setup layout (a) top view, (b) side view.

3.2 Data Transmission Component (Data Logger)

For collecting the PV panel output from the field we had to develop a data logger. The main purpose of using this system is to collect data continuously. For ensuring the availability of data this system also able to save data locally and upload the collected the in the cloud storage.

3.2.1 Data Transmission Technique

All of the panels' outputs, as well as the surrounding conditions data, must be monitored continuously every 2-3 minutes for our research. A data logging system will be introduced to collect data from the site every two minutes. We used a data logger system that we developed in-house for this purpose. In Fig.3.6, we can see the datalogger collects the output of the PV panels and then uploads the output through the *ThingSpeak* cloud server. Then by using MATLAB code we downloaded the output data and have done further analysis.

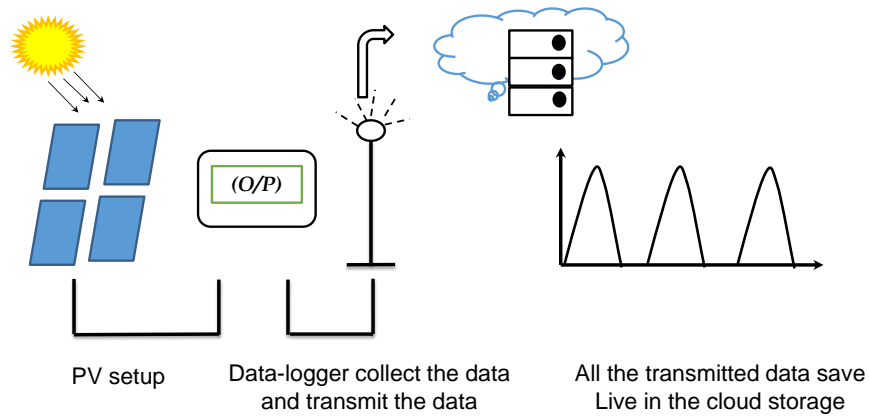


Fig. 3.6 Data Acquisition through Cloud Server.

3.2.2 Data Logger in PCB

The system was first tested in the breadboard before being deployed on-site for outdoor measurements with a PCB-designed data logger circuit (Fig.3.7 (a)). The datalogger circuit Arduino, analog pin received the analog output from the PV panels through the load circuit. Fig.3.7 (b), shows the load circuit of the datalogger whose main component is 1Ω ceramic resistance. The load circuit positive terminal is connected to the PV module's positive terminal and the negative terminal of the PV module is connected to the load circuit negative terminal. We used a 1Ω ceramic resistance as a load because we can calculate the short circuit current of the PV module approximately by using Ohm's law, $V=IR$. If $R = 1\Omega$, then $V=I$. So, the voltage we measured is close to the short circuit current of the PV module. Fig.3.7 (c), represents the connection of the PV modules with the load circuit and the data logger which is in house condition. This data logger has been developed in a collaboration with Khan SLR group Research Assistant Jabir Bin Jahangir.

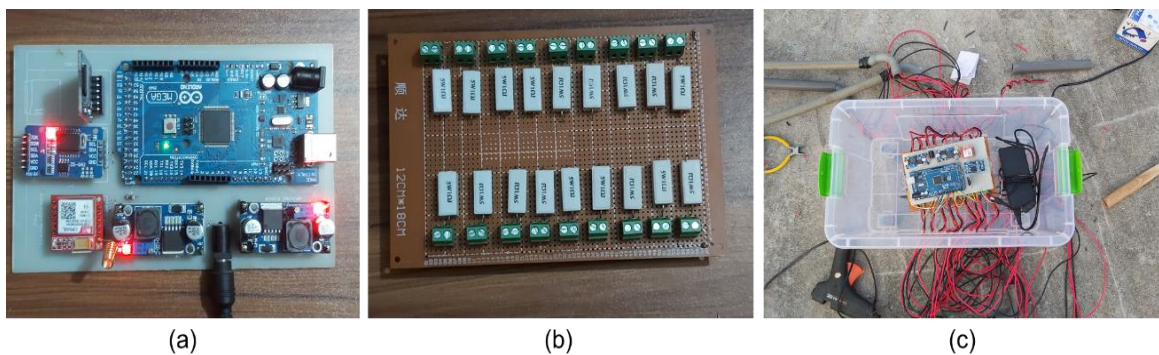


Fig. 3.7 Datalogger (a) PCB design setup, (b) Load circuit, and (c) Datalogger in house setup.

3.3 PV Module Connection

During the research work we observed the soiling effect for both monofacial and bifacial experimental setup. For bifacial panel we used to PV module back to back that represents as bifacial PV panel. The PV module connection with load circuit with both monofacial and bifacial panels are different.

3.3.1 Monofacial PV Panel Connection

The Monofacial PV panel setup has six tilt angles. Each tilt angle has three PV modules. Each tilt angle has two cleaning cycles. Fig.3.8, shows the connection for monofacial PV panel. Where, DC, WC, and MC mean daily, weekly, and monthly clean panels. In this connection, all modules ground is connected together along with the datalogger microcontroller ground. PV modules (+ve) terminal wire then connected to datalogger ADC. Here, in the load circuit, 1 Ohm ceramic resistance has been used. According to the Ohms law, $V=IR$, where, we know $R = 1\Omega$, therefore, we got $V=I$ (approximately), therefore, the voltage that we are measuring using the datalogger is actually the short-circuit current (I_{sc}). Table 3.1 shows the technical parameters of the PV panel that has been used in the experiment.

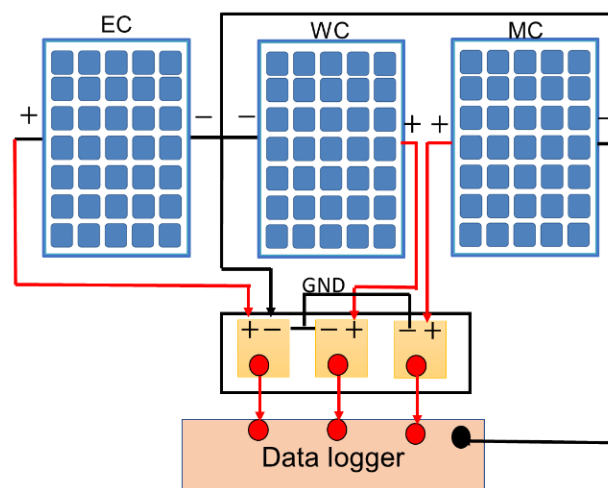


Fig. 3.8 PV Modules Connection for monofacial PV panel Experimental Setup.

Table 3.1 Electrical Parameter for Monofacial PV Panel Specification

| Items | Symbols | Values |
|-----------------------|-----------|---------|
| Maximum power | P_{max} | 20 W |
| Operating voltage | V_{mp} | 18 V |
| Operating current | I_{mp} | 1.18 A |
| Open circuit voltage | V_{OC} | 21.01 V |
| Short circuit current | I_{SC} | 1.22 A |

3.3.2 Bifacial PV Panel Connection

The bifacial PV panel setup has three tilt angles. Each tilt angle has two PV modules. Each tilt angle has two cleaning cycles. Fig.3.9, shows the connection for the bifacial PV panel. In order to measure the output of each face, we used two back-to-back panels to model a bifacial panel for the bi-facial PV panel experiment. The significance of this model is that we can assess each panel's soiling rate individually. Since both panels have the same efficiency so we can compare their output based on their performance. Where, FP means front panel and RP means rear panel. Table 3.2 shows the technical parameters of the PV panel that has been used in the experiment.

Table 3.2 Electrical Parameter for Bifacial PV Panel Specification

| Items | Symbols | Values |
|-----------------------|-----------|--------|
| Maximum power | P_{max} | 30 W |
| Operating voltage | V_{mp} | 17.2 V |
| Operating current | I_{mp} | 1.74 A |
| Open circuit voltage | V_{OC} | 21.6 V |
| Short circuit current | I_{SC} | 1.93 A |

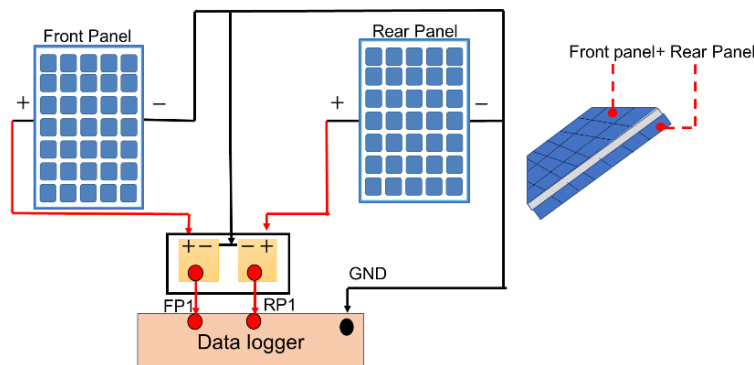


Fig. 3.9 PV Modules Connection for bifacial PV panel Experimental Setup.

3.4 Experimental Setup in Testing Site

Fig.3.10 shows the experimental setup of the mono-facial PV panel experimental setup. There is a total of six different tilt angles PV modules settled down in the southern face consecutively. Fig.3.11 (a) illustrates the experimental setup of the bi-facial PV panel experimental setup. There are three distinct tilt angles PV module settle in the southern face. Fig.3.11 (b) represents the way of making bi-facial PV panels by using two different PV modules. By this, we can easily assess the generated energy of the front and rear PV panels separately.

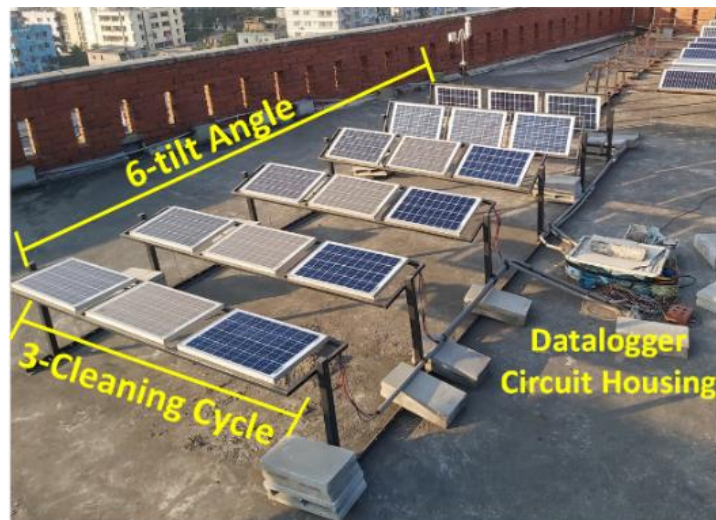


Fig. 3.10 Experimental setup of mono-facial PV panels.



Fig. 3.11 Experimental setup of, (a) bi-facial PV panels, (b) bifacial PV modules.

3.5 Cleaning Procedure to Mitigate the Soiling

Soiled panel output can be retrieved by cleaning the PV panel immediately. Cleaning intervention on PV panels can minimize the soiling effect. The cleaning procedure of PV farms can be categorized into two types-(1) natural cleaning procedure, and (2) artificial cleaning procedure.

Natural cleaning procedures are rainfall, wind, and gravity effect. Rainfall is a very good type of natural cleaning procedure. Light rainfall is not enough to clean the soiled PV panel. Sometimes light rainfall can be the cause of decreasing PV panel performance [51]. However, heavy rainfall or moderate rainfall can clean the soiled PV panel clearly to retrieve soiled panel performance. There is also a significant relationship between the PV panel tilt angle and rainfall for cleaning the soiled PV panel. On the other hand, low wind speed also can cause dust accumulation on the PV panel surface [52]. The good thing about the natural cleaning procedure is that it does not add any extra cost for the cleaning procedure. But the drawback is that the natural cleaning procedure is not planned and scheduled.

3.5.1 Manual Cleaning

The manual cleaning procedure of PV panel is a conventional procedure of PV panel cleaning method. Manual cleaning has good cleaning results. Using manual cleaning process difficult dust accumulation for example non-uniform soiling, bird-droppings can be removed easily. The manual cleaning is actually human aid cleaning with brush and water. Manual cleaning cost varies from region to region. Also vast PV installed capacity will cost very high expense due to the manual cleaning procedure.

3.5.2 Automated Cleaning Procedure

Automated cleaning or machine cleaning procedure are mechanized approaches to clean the soil PV panel with the help of robotic equipment. Now a days, water based automatic cleaning process are used but it needs more water than the manual cleaning procedure. Mechanized automated cleaning approaches need energy consuming devices which also need regular maintenance, which add another cost [53]. So technically behind and having water scarcity regions PV farm are not likely to adopt automated cleaning procedure. In south Asian region most of the PV power plant adapt manual cleaning procedure instead of automated cleaning procedure.

After justifying the prior literature regarding the PV panels cleaning intervention, we likely to adopt manual cleaning procedure (soft cloth and water) for cleaning the PV panels of our infield experimental setup.

3.6 Methodology of Analysis

3.6.1 Measurements and Integrated Input/output Data

From January 1, 2022, to March 26, 2022, we collected and saved panel short circuit data every 2 minutes for 6 distinct tilts and 3 separate cleaning cycles at each tilt (a total of $6 \times 3 = 18$ panels). The following are the three cleaning cycles that were chosen:

- 1) Cleaning every day (EC)
- 2) Cleaning intervention once a week (WC)
- 3) Cleaning intervention once a month (MC)

Similarly, we have collected data for a bi-facial PV setup for 3 distinct tilts and 1 cleaning cycle at each tilt (a total of $3 \times 4 = 12$ panels).

3.6.2 Performance Ratio (PR)

A data logging system was used to measure short circuit currents (I_{SC}) from the each module, every two minutes. The I_{SC} values are mapped to maximum power point output P_{mp} and then integrated to obtain the daily energy yield $E(t)$. For a front (F)-facing panel at tilt β , we represent the daily energy as $E_{\beta 0}^{(F)}$ and $E_{\beta}^{(F)}$ for clean and unclean cases respectively. We define Performance Ratio (PR) as the ratio of the daily output of a soiled (unclean) panel to that of a clean panel as follows:

$$PR_{\beta}^F(t) = \frac{\text{Daily energy of soiled panel, } E_{\beta}^{(F)}(t)}{\text{Daily energy of clean panel, } E_{\beta 0}^{(F)}(t)} \quad (3.1)$$

For the bi-facial PV panels experiment, the performance ratio (PR_{β}^B) of the back (B)-facing panels are similarly calculated.

3.6.3 Soiling Rates (SR)

To calculate the soiling rate a_β (/day) between cleaning interventions, we fit the $PR_\beta(t)$ data with the empirical soiling loss model: $A \exp(-a_\beta t)$.

3.6.4 Revenue and Cleaning Cycle Calculation

The mean daily cash-inflow from a panel is $R \times \bar{E}_\beta$. Here R is the tariff rate, and the mean daily energy produced is

$$\bar{E}_\beta = \begin{cases} \frac{1}{N_{\text{days}}} \sum [E_\beta^{(F)}(t) + E_\beta^{(B)}(t)], & \text{for bifacial} \\ \frac{1}{N_{\text{days}}} \sum [E_\beta^{(F)}(t)], & \text{for monofacial} \end{cases} \quad (3.2)$$

These panels have their corresponding soiling rates a_β . The earned revenue would be calculated by subtracting the cleaning costs from the cash-inflow cash we can find the rated revenue $R \times \bar{E}_{\beta 0}$ by considering the soiling-free (clean) panel outputs.

With a cleaning cycle of t_c days, we can numerically predict the mean daily revenue from monofacial the pans follows [4]:

$$\text{Rev}_\beta^{\text{mono}} = R \bar{E}_{\beta 0}^{(F)} \times \left(1 - \frac{1}{2} a_\beta t_c - \frac{C}{R \bar{E}_{\beta 0}^{(F)}} \frac{1}{t_c} \right) \quad (3.3)$$

Here, $\bar{E}_{\beta 0}^{(F)}$ is the mean daily energy output of a soiling-free panel (front-facing) and C is the cost for each cleaning cycle. Typically, we expect minimal soiling on the back-faces of a bifacial panel [35]. Therefore, outputs from the clean and unclean back-faces are equal $\bar{E}_\beta^{(B)} = \bar{E}_{\beta 0}^{(B)}$. Finally, as we expect almost no cleaning costs at back faces, we can expand Eq. (3.3) for bifacial panels:

$$\text{Rev}_\beta^{\text{bi}} = R \bar{E}_{\beta 0}^{(F)} \times \left(1 - \frac{1}{2} a_\beta t_c - \frac{C}{R \bar{E}_{\beta 0}^{(F)}} \frac{1}{t_c} \right) + R \bar{E}_{\beta 0}^{(B)} \quad (3.4)$$

We optimize the cleaning cycle by numerically maximizing Rev_β versus t_c . Note that, a_β , $\bar{E}_{\beta 0}^{(F)}$, and $\bar{E}_{\beta 0}^{(B)}$ are calculated from our experimental measurements. In Eqs. (3.3) and (3.4), we use R in USD/kWh, C in USD/Wp, a_β in /day, and $\bar{E}_{\beta 0}$ in kWh/Wp.

Using the soiling rates for each panel tilt, we have the economic analysis. We will calculate the losses at different cleaning cycles for soiling rates at each tilt. By balancing the electricity sold and cleaning costs we can maximize the revenue.

3.6.5 Revenue Analysis Considering Whole Year

If we multiply the full year energy (kWh) with tariff rate and deduct the total cleaning cycle cost then we can calculate the whole year revenue for the particular tilt angle PV panels.

$$R_v = E_{full\ year} \times R - N_{days} \times C \quad (3.5)$$

Here, $E_{full\ year}$ is the energy of full year that has been produced by the specific PV panel in (kWh), R is the tariff rate in US-¢ (US-Cent), N_{days} is the number of cleaning intervention done and C represents the cleaning cost of each cleaning intervention.

CHAPTER 4

RESULT ANALYSIS AND DISCUSSION

This chapter presents the analysis of the experimental data. First, we calculate the soiling rates of monofacial and bifacial panels. We use the monofacial soiling rates for the economic analysis of the monofacial setup, and the bifacial soiling rates for the economic analysis of the bifacial setup. Next, we examine the angle dependence of soiling rates and establish an empirical relationship. Then, we conduct the economic analysis of both PV panel setups and determine the optimum cleaning cycle for each tilt angle to maximize the revenue. Finally, we compare the revenue for different cleaning cycles.

4.1 Analysis of Mono-Facial PV Panels

4.1.1 Evaluating the Soiling Rate of Monthly Cleaned PV Panels at Various Tilt Angles

The experiment has been conducted in winter from 1st, January 2022, and 26th March 2022. During the experiment, one mono-facial configuration was cleaned daily. The other two sets cleaning cycle1 named (C1) have been cleaned once a week, and cleaning cycle 2 named (C2) cleaned once a month.

The performance ratio (PR) of a monthly cleaned panel of mono facial setup 0°, 10°, 20°, 30°, 60°, and 90° tilt angle PV panel is represented in Fig.4.1. Here, we can see a dashed blue line indicates the rainfall event on the testing site. We found that the soiled panel became clean and produced the same output as the clean panel after a sufficient rainfall event. However, if the rain was too light, the solar panel did not get cleaned effectively. The green dashed line represents the manual cleaning event that has been done at the beginning of January, and February. Fig.4.1 shows that the performance ratio of PV panels almost linearly decreased over time.

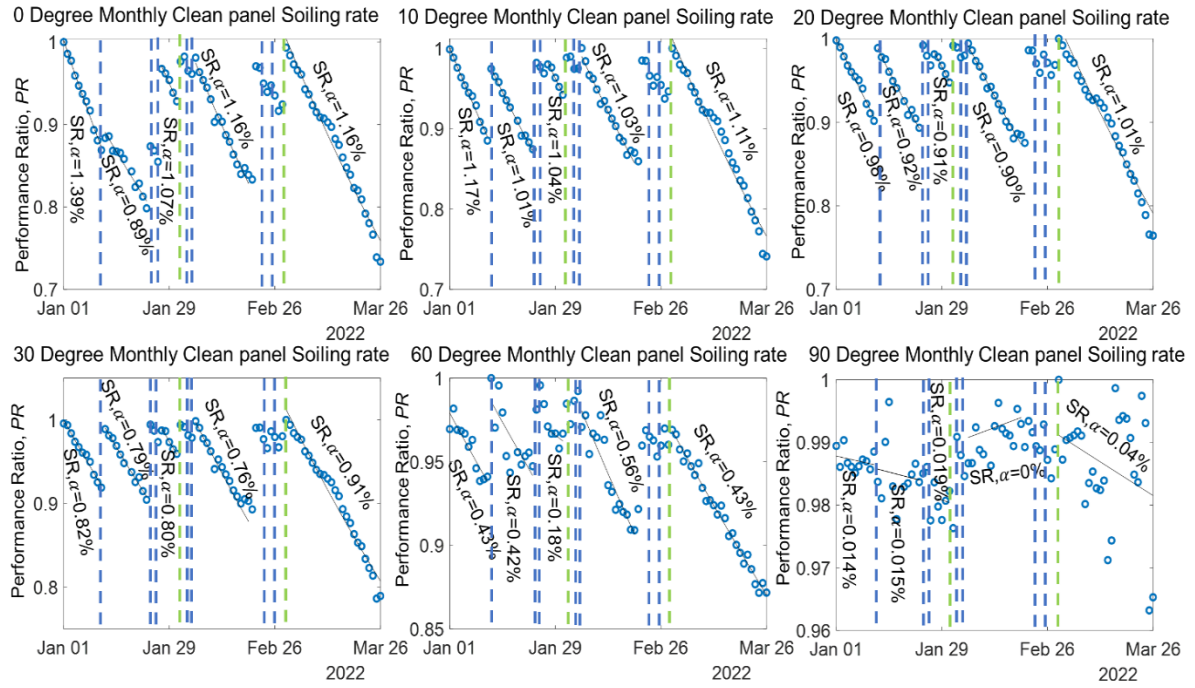


Fig. 4.1 Soiling rates between cleaning cycles and rainfall of mono-facial monthly clean PV panels.

Table 4.1 Monthly Cleaned Panel Soiling Rate (%)

| Date | Jan (1 to 11) | Jan (12 to 23) | Jan (27 to 31) | Avg. Of Jan | Feb (6 to 19) | March (1 to 26) |
|------------------------|------------------|-------------------|-------------------|----------------|------------------|--------------------|
| Tilt Angle (β) | | | | | | |
| 0 | 1.39 | 0.89 | 1.07 | 1.1167 | 1.16 | 1.12 |
| 10 | 1.17 | 1.01 | 1.04 | 1.0733 | 1.03 | 1.11 |
| 20 | 0.98 | 0.92 | 0.91 | 0.9367 | 0.90 | 1.01 |
| 30 | 0.82 | 0.79 | 0.80 | 0.8033 | 0.76 | 0.91 |
| 60 | 0.43 | 0.42 | 0.18 | 0.3433 | 0.56 | 0.43 |
| 90 | 0.014 | 0.015 | 0.019 | 0.0160 | 0.00 | 0.04 |

In table-4.1, the soiling rate of the monthly clean panel has mentioned. In the case of January month, there had been rained on the 11th, 24th, 25th, and 26th of January. Therefore, we calculated the soiling rate for that month at a 3-time window, and for determining the soiling rate for January, we averaged the soiling rates for January. For February month 1st to 5th, and the 20th to 26th date there was a rain event that occurred. Therefore, in calculating the soiling rate for February, we skipped the rainy day data. For March, we have calculated the whole month's soiling rate from the 1st to the 26th of March.

4.1.2 Evaluating the Soiling Rate of Weekly Cleaned PV Panels at Various Tilt Angles

Fig.4.2 mentions the soiling rate of the weekly clean panel of 0°, 10°, 20°, 30°, 60°, and 90° tilt angles. These panels had been cleaned every week. In the fig.4.2. dashed blue line indicates the rainfall event on the testing site. The green dashed line represents the manual cleaning event that has been done every week of January, February, and March. Fig.4.2 shows the same trend as Fig.4.1, therefore for further calculation of economic analysis, we will consider only the soiling rate of the monthly clean panel.

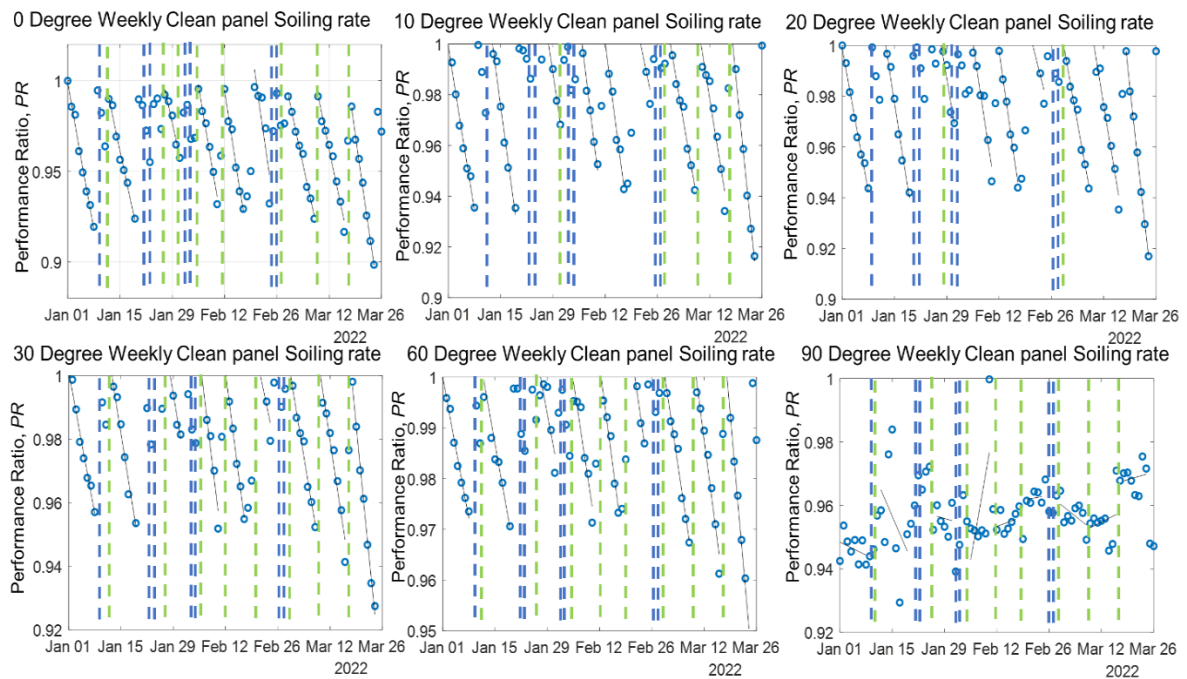


Fig. 4.2 Soiling rates between cleaning cycles and rainfall of mono-facial weekly clean PV panels.

Table 4.2 Weekly Cleaned Panel Soiling Rate (%)

| Date | 0 Degree | 10 Degree | 20 Degree | 30 Degree | 60 Degree | 90 Degree |
|----------------|----------|-----------|-----------|-----------|-----------|-----------|
| Jan (1 to 8) | 1.21 | 0.96 | 0.83 | 0.66 | 0.40 | 0.06 |
| Jan (12 to 17) | 1.02 | 1.13 | 0.97 | 0.76 | 0.42 | 0.28 |
| Jan (27 to 31) | 0.96 | 1.001 | 0.89 | 0.71 | 0.40 | 0.04 |
| Jan Average | 1.063 | 1.030 | 0.897 | 0.710 | 0.407 | 0.127 |
| Feb (5 to 10) | 1.27 | 1.23 | 0.995 | 1 | 0.50 | 0.00 |
| Feb (12 to 17) | 1.39 | 1.17 | 1.07 | 0.94 | 0.57 | 0.00 |
| Feb (20 to 24) | 1.48 | 0.72 | 0.59 | 0.56 | 0.51 | 0.00 |
| Feb Average | 1.38 | 1.04 | 0.885 | 0.833 | 0.527 | 0.00 |
| Mar (1 to 8) | 1.002 | 0.89 | 0.84 | 0.73 | 0.50 | 0.098 |
| Mar (9 to 16) | 1.04 | 0.94 | 0.92 | 0.81 | 0.58 | 0.00 |
| Mar (20 to 24) | 1.54 | 1.53 | 1.41 | 1.24 | 0.86 | 0.00 |
| Mar Average | 1.194 | 1.120 | 1.057 | 0.927 | 0.647 | 0.0327 |

The table-4.2 shows the soiling rate of the weekly clean panel 0°, 10°, 20°, 30°, 60°, and 90° tilt angles. For this set of PV panels, the cleaning intervention was taken once every week. Between each cleaning intervention, we calculated the soiling rate. After that for each month soiling rate has been calculated by averaging of specific tilt angle soiling rate.

4.2 Rainfall Data during the Experiment

Figure 4.3 shows the rainfall events that occurred during the experiment period. The data covers the months of January to March 2022, which is normally a dry season. However, there were some rainfall events, especially in January, when the amount of rainfall was high. The rainfall decreased gradually in February and March.

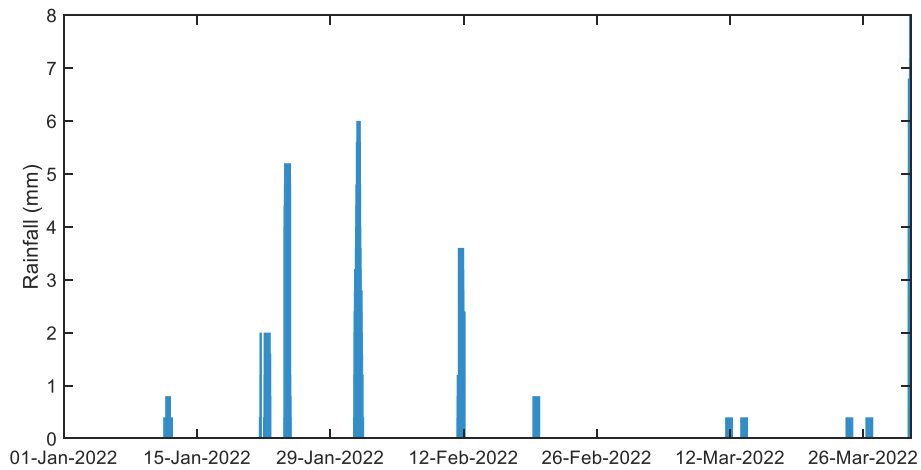


Fig. 4.3 Rainfall Data of January to March 2022.

The effect of rainfall on the cleaning performance of the PV panel was investigated. The results showed that there was a threshold value of rainfall intensity that ensured effective cleaning of the panel. Below this threshold, the panel remained dirty after the rainfall event.

4.3 Observing Angle Dependence of Different Tilt Angles Soiling Rate

Fig.4.4, shows the angle dependence of different tilt angles (0°, 10°, 20°, 30°, 60°, and 90°) monthly clean PV panel soiling rates for the January, February, and March months. The dashed violate line shows the average of the soiling rate for these three different months. The average soiling rates are 1.13, 1.07, 0.95, 0.82, 0.44, and 0.019%/day respectively. It also shows the angle dependence of different tilt angles (0°, 10°, 20°, 30°, 60°, and 90°) weekly clean PV panel soiling rates for the mentioned months. WC and MC panel also shows the

same. The soiling rate for weekly clean panels is, 1.21, 1.06, 0.95, 0.82, 0.53, 0.9053%/day which shows an almost similar soiling rate as monthly clean panels soiling rates. Fig.4.4, indicates that the soiling rate of PV panels proportionally depends on the tilt angles. For lower tilt angles, the soiling rate is high for higher tilt angles the soiling rate is less which is expected.

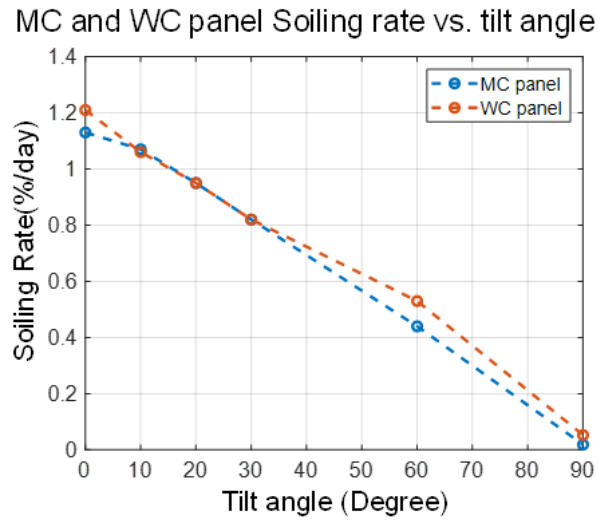


Fig. 4.4 Angle dependence of different PV panels soiling rates of monthly and weekly cleaned panel.

Here we can see that soiling rates between two different cleaning cycles are almost the same. Interestingly, we observed that the soiling rate of 0° weekly clean panel is higher than the monthly clean panel. But the soiling rate of 10°, 20°, and 30° panels are the same. After that, for 60° and 90° tilt angle PV panels, the soiling rates of the weekly clean panel is higher than the monthly clean panel. Since the differences in soiling rates between the two different cleaning cycles are very less, therefore, evaluating of the techno-economic analysis we considered the average soiling rates of the monthly clean panels.

4.4 Empirical Approach of Angle Dependence of Soiling Rate

From the experimental result, we observed that the angle dependence of PV panel tilt angles and soiling rates were almost linear. Therefore, we average the monthly cleaned (MC) Panel soiling rate and then fitted the curve linearly. From this curve we got a straight line equation.

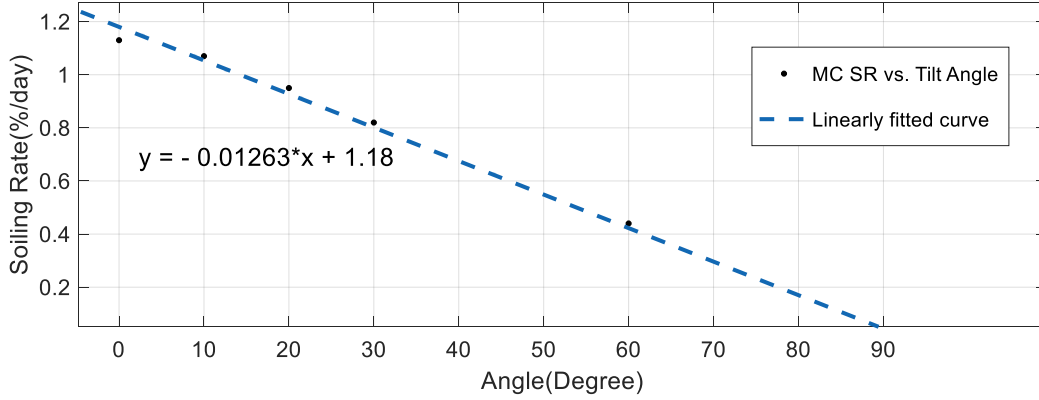


Fig. 4.5 Angle dependence of PV panels tilt angle relationship with soiling rate through an empirical approach.

Fig.4.5, shows that the fitted curve is straight line. From this curve we can easily derive an equation.

The linear model of angle dependence of PV panels tilt angle with soiling rates:

$$SR = P_1\beta + P_2 \quad (4.1)$$

Coefficients

$$P_1 = -0.01263; \quad P_2 = 1.18; \quad \beta = PV \text{ panel tilt angle}$$

Figure 4.5 shows the relationship between the soiling rate and the tilt angle of the PV panels, based on an empirical approach. The figure shows a linear fit of the average soiling rate, which follows a decreasing trend. The equation of the fit can be used to estimate the soiling rate for any specific location, where SR is a function of β . To do this, we need to know the soiling rate for the 0° tilt angle first. Then we can use equation (4.1) with the values of P_1 and P_2 to predict the soiling rate for other tilt angles of PV panels. Equation (4.1) can be applied to our experiment location or Bangladesh to determine the soiling rate.

Eqn.4.1, shows the straight line equation, $y = mx + c$. We can also generalize the eqn.4.1 as the following eqn.4.2,

$$(SR_{\beta}) = a(0) \times \left(1 - \frac{\beta}{90}\right) + a(90) \quad (4.2)$$

This equation allows us to calculate the soiling rate for any tilt angle of PV panels for a specific location if we know the soiling rate for the 0° and 90° tilt angles. In most cases, from our experiment, we observed that the soiling loss for the 90° tilted PV panel was zero. Therefore, we can set the value of $a(90)$ to zero.

4.5 Optimum Cleaning Cycle of Different Tilt Angle

For the numerical analysis with varying cleaning cycles, we use the mean soiling rates (averages over the fitting intervals) for each tilt β . Fig. 4.6 illustrates the revenue versus cleaning cycle for both mono facial PV panels. We set cleaning cost, $C = 5000$ BDT/MW, and tariff rate, $R = 8.50$ BDT/kWh. These are average values for Asia estimated from Ref. [4]. The plots in Fig. 3 are obtained using experimentally measured a_{β} , and $\bar{E}_{\beta 0}^{(F)}$ values in EQs. (3.2) and (3.3). The cleaning cycle t_c discussed here is for the front face.

Table 4.3 Techno-Economic Analysis Summary of Monofacial PV setup

| Panel tilt, β | Clean panel output (W-h/W _p) | Soiling rate, α (%/day) | Optimum t_c (Days) |
|---------------------|--|--------------------------------|----------------------|
| 0° | 3.68 | 1.13 | 4 |
| 10° | 4.08 | 1.07 | 4 |
| 20° | 4.39 | 0.95 | 4 |
| 30° | 4.53 | 0.82 | 4 |
| 60° | 4.05 | 0.44 | 6 |
| 90° | 2.79 | 0.019 | >30 |

From the experiment, we assessed the energy production and soiling rate of the panels at various tilt angles. Following that, we numerically estimated the optimum cleaning cycle for each tilt angle using these data. As listed in Table-4.3, the optimum cleaning cycles for $\beta = 0^\circ, 10^\circ, 20^\circ, 30^\circ, 60^\circ$, and 90° tilted panels are 4, 4, 4, 4, 6, and >30 days respectively.

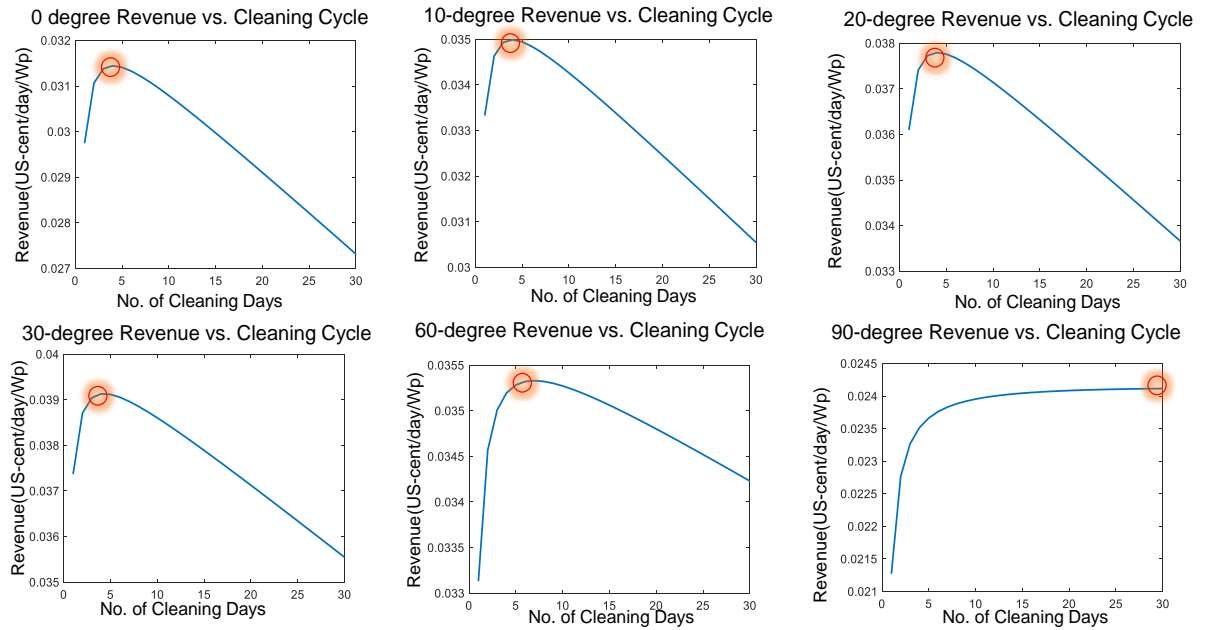


Fig. 4.6 Relationship between revenue and cleaning cycle of different tilt angles monofacial PV panel.

According to Fig.4.5, the solar panels that are optimally cleaned and tilted at 30° generated the highest revenue. We can also observe that the PV panel with a 90° tilt angle has the longest optimal cleaning cycle, which is more than 30 days. This is because the vertical position of the PV panel minimizes the soiling loss. Therefore, the 90° tilted PV panel requires less frequent cleaning than the other tilt angles.

4.6 Energy Generation Comparison between Different Tilt Angles

Fig.4.7 shows the energy output of different tilt angles of the PV panels. The 30° tilted PV panel had the highest energy output, which was suitable for this location (23.7685° N, 90.4255° E). The figure also shows that the daily cleaned panel had the highest energy output for each tilt angle, followed by the weekly cleaned panel and then the monthly cleaned panel. This was due to the effect of soiling, which accumulated more on the monthly cleaned panel than on the weekly cleaned panel.

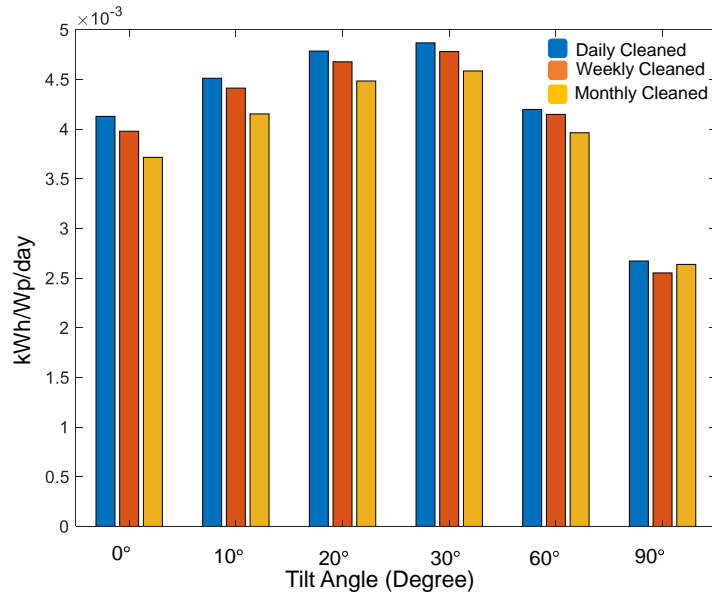


Fig. 4.7 Energy generation of PV panel in different tilt angles.

The daily cleaned panel was free of soiling and had the highest energy output for each tilt angle. The weekly and monthly cleaned panels were cleaned once a week and once a month, respectively. Therefore, the weekly cleaned panel had less soiling accumulation than the monthly cleaned panel and generated more energy.

However, for the 60° and 90° tilted panels, there was a slight difference between the weekly and monthly cleaned panels due to the higher tilt angle. Also, there was a technical issue with the 60° tilted PV weekly cleaned panel during the experiment, which resulted in higher energy output than the monthly cleaned panel.

4.7 Revenue Analysis for Monofacial PV Experimental Setup

During the economic analysis we considered four set of PV panel. Soiling less PV panel, daily, weekly, and monthly cleaned PV panel. We consider there no soil accumulates on soiling less PV panel. The total duration of the experiment from 1st January, 2023 to 26th March, 2023, total 84 days.

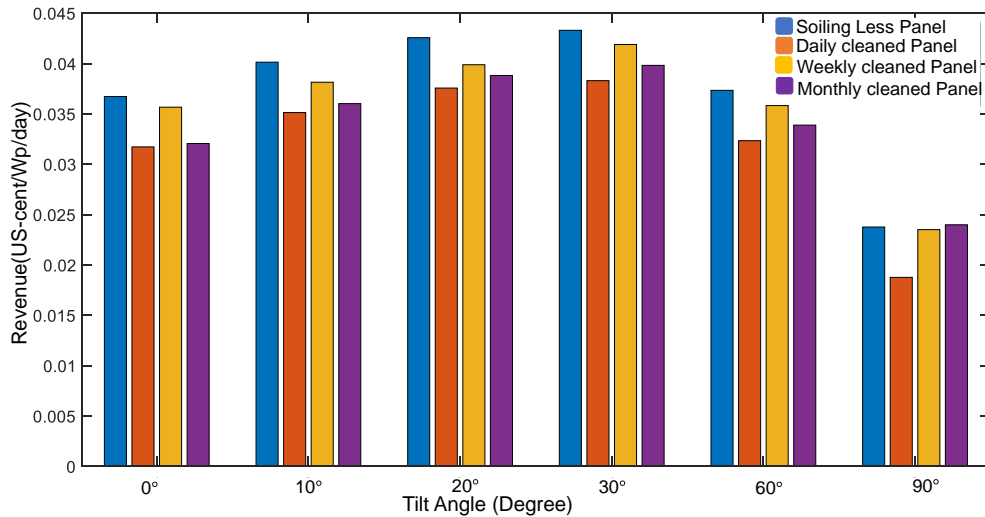


Fig. 4.8 Revenue comparison of soiling less, daily, weekly and monthly cleaned panel.

Figure 4.8 shows the mean daily revenues of the different PV panels during the experiment. The soiling-less PV panel had the highest revenue because it did not incur any cleaning costs. The revenue was calculated by multiplying the energy output and the tariff rate per kWh. The daily cleaned panels had lower revenue than the weekly and monthly cleaned panels because they required more cleaning interventions. The monthly cleaned panels had higher revenue than the daily cleaned panels because they only needed three cleaning interventions during the experiment, one at the beginning of each month. The weekly cleaned panels had the highest revenue among the cleaned panels because they were cleaned optimally. As shown in section 4.5, the optimum cleaning frequency for each tilt angle was 4 to 6 days, which was close to the weekly cleaning schedule. The weekly cleaned panels were cleaned 12 times in three months.

It is interesting to note that the daily cleaned panel, which had the highest energy output in Figure 4.7, had lower revenue than the weekly and monthly cleaned panels because of the high cleaning cost. The monthly cleaned panel, which had the lowest cleaning cost, had lower revenue than the weekly cleaned panel because of the high soiling accumulation. Therefore, for a PV farm, only the optimally cleaned PV panels can maximize the revenue by balancing the revenue and cleaning cost. Fig.4.8 shows that the 30° tilted PV panel had higher revenue than the other tilted PV panels for all cleaning schedules.

It should be noted that the revenue calculations for the weekly cleaned panels did not consider the rainfall events, while the monthly cleaned panels experienced several rainfall events in the same month. However, the weekly cleaned panels still had higher revenue than

the monthly cleaned panels. This suggests that the rainfall events during the experiment were not enough to offset the cleaning costs.

4.8 Analysis of Bifacial PV Panels

4.8.1 Evaluating the Soiling Rate of Bi-Facial PV Panels at Various Tilt Angles

This experiment has been conducted in winter from 12th December 2021 to 14th February 2022. During the experiment, one set of bifacial panel configurations have been cleaned daily. The other set (unclean panels) was left outdoors to accumulate dust. There were five rain events during the experimentation when the unclean panels were naturally cleaned fully or partially. Additionally, these ‘unclean panels’ were manually cleaned on 1st February 2022.

The performance ratio ($PR_{\beta}^F(t)$) of the front faces of the 0°, 20°, and 30° tilted unclean PV panels are shown in Fig. 4.9. Some of the data from 15 January to 20 January 2022 are missing due the data logger downtime. In these figures, the solid vertical lines indicate rain and dashed vertical lines indicate manual cleaning. The soiling rate (SR, a_{β}) of a panel has been determined from the slope of PR_{β}^F between two cleaning interventions (rain or manual cleaning).

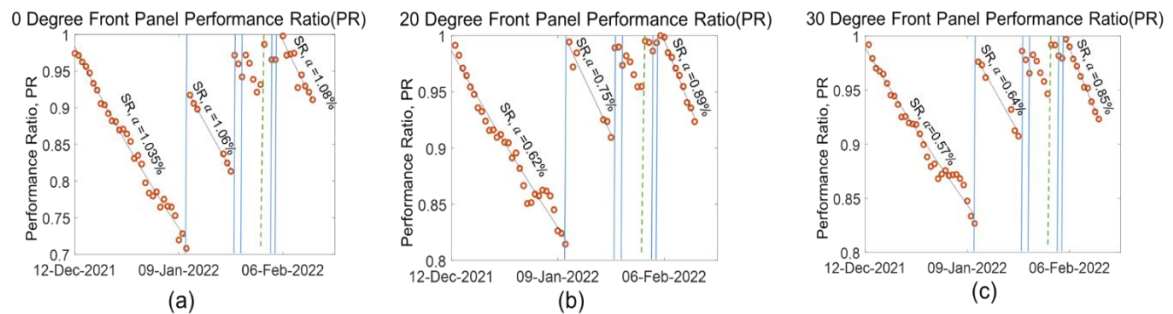


Fig. 4.9 Soiling rates between cleaning cycles and rainfall (a) 0-degree tilt angle, (b) 20-degree tilt angle, and (c) 30-degree tilt angle.

Fig. 4.9 shows that the performance ratio of PV panels almost linearly decreased with respect to time. Therefore, the accumulation of soiling on PV panels decreases the PV panel’s generation proportionally. On the 11th of January 2022, rainfall completely cleaned the uncleaned panels. Therefore, a good amount of rain can clean the uncleaned panel properly, and cleaning expenditures can be avoided on such days. We observe that the soiling rates vary within a few weeks. Finally, as expected, the soiling rate is higher at lower

tilt angles. We calculated the performance ratio PR_{β}^B for the back-facing panels as well (not presented here). We observed no degradation in the mean PR_{β}^B indicating no measurable soiling on the back faces.

4.8.2 Optimum Cleaning Cycle of Bifacial PV Panels

For the numerical analysis with varying cleaning cycles, we use the mean soiling rates (averages over the fitting intervals) for each tilt β . Fig. 4.10 illustrates the revenue versus cleaning cycle for both monofacial and bifacial PV panels. We set cleaning cost, $C = 0.03$ USD/kWp, and tariff rate, $R = 0.0895$ USD/kWh. These are average values for Asia estimated from Ref. [4]. The plots in Fig. 4.10 are obtained using experimentally measured a_{β} , $\bar{E}_{\beta 0}^{(F)}$, and $\bar{E}_{\beta 0}^{(B)}$ values in Eqs. (3.2) and (3.4).

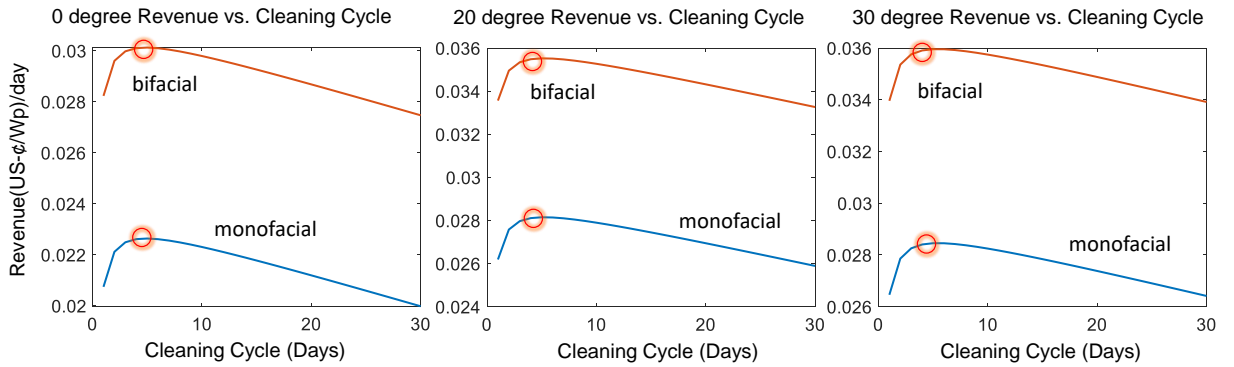


Fig. 4.10 Relationship between revenue and cleaning cycle, (a) 0-degree tilt angle, (b) 20-degree tilt angle, and (c) 30-degree tilt angle.

As discussed earlier, the soiling effect on the rear side of bifacial panels is zero. The cleaning cycle t_c discussed here is for the front face. As listed in Table I, the optimum cleaning cycles for $\beta = 0^\circ$, 20° , and 30° tilted panels are 5, 5, and 6 days respectively. From Fig. 4.10, we also see that optimally cleaned, 20° tilted panels may yield the highest revenue.

We found that the optimum cleaning cycle for bifacial PV panels is the same as for monofacial PV panels. This is because bifacial PV panels only experience soiling on the front side. So they need to be cleaned as often as monofacial PV panels. However, we suggest that the rear side of bifacial PV panels should be cleaned once a month to prevent cementation.

Fig. 4.10 indicates that, compared to monthly cleaning, optimal cleaning can increase the revenue by 5.5-8% (or 7.5-10%) for bifacial (or mono facial) panels. We also observe a 27-34% increase in revenue for bifacial compared to mono facials.

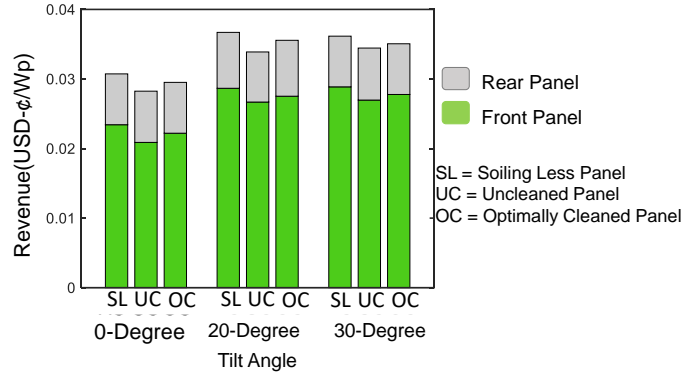
Table 4.4 Techno-Economic Analysis Summary of Bifacial PV setup

| Panel tilt, β | Clean panel output (W-h/Wp) | | Soiling rate, a (%/day) | Optimum t_c (Days) |
|---------------------|-----------------------------|---------------------------|---------------------------|----------------------|
| | Front, $E_{\beta 0}^{(F)}$ | Back, $E_{\beta 0}^{(B)}$ | | |
| 0° | 2.62 | 0.837 | 1.058 | 5 |
| 20° | 3.203 | 0.823 | 0.753 | 5 |
| 30° | 3.23 | 0.837 | 0.687 | 6 |

Table-4.4 also presents the clean bifacial panel output. Depending on the tilt, the back face can collect a fraction of diffuse sunlight and the albedo. The back-face light collection will be determined by the view factor from the panel face to the sky and the ground [54]. For sufficiently elevated standalone panels, the back-face collection during Dec.-Feb. in Dhaka is predicted to be comparable for 0°, 20°, and 30° tilts [55]. This is consistent with our measurements. We measured the energy output and soiling rate of the panels at different tilt angles from the experiment. Then we used these data to estimate the optimal cleaning cycle for each tilt angle numerically. We found that for 0°, 20°, and 30° tilts the optimum cleaning cycle is 5 to 6 days.

4.9 Revenue Analysis for Bifacial PV Experimental Setup

During this set of experiment we have considered 3 set of cleaning cycle, always cleaned, uncleaned and optimally cleaned. Fig.4.11, shows the mean daily revenues of the different PV panels during the experiment.



27

Fig. 4.11 Revenue comparison of uncleaned and optimally cleaned panel.

As expected, the soiling less panel (SL) panels yield higher than the unclean (UC) panels. These are calculated from the energy production measured in the experiments. The revenue from the optimally cleaned (OC) panels is also shown here. Note that, the numerical calculations for OC panels neglect rainfall, whereas the measured UC panels had 5 rain events. Even then the revenue from OC panels is higher than that of UC. This indicates that the few rainfall events during the experiment did not have a strong enough impact to outweigh the cleaning costs.

CHAPTER 5

NON-UNIFORM SOILING ECONOMIC ANALYSIS

Soiling can degrade the performance of photovoltaic (PV) panels over time. Some cleaning techniques may not remove the dust and particle evenly, causing partial or non-uniform shading on the PV panel. This can reduce the output power and lifetime of the panel, affecting the economics of the PV farm. We developed a simple I-V scanner to measure the changes in the I-V and P-V curves of the PV panel under different shading scenarios. We used controlled experiments to emulate and analyze the effects of bird-droppings and uneven soiling on the PV panel surface.

This chapter investigates the impact of partial or non-uniform shading on PV panels due to soiling or bird droppings. We use the maximum power point (MPP) of the PV panels to compare their performance under different shading scenarios. We show how soiling bands or bird droppings on the panel edges can reduce the output of the panel array and suggest ways to optimize solar farm operation. We also design a simple and portable I-V scanner to measure the changes in the I-V characteristics of a PV module in real-time.

Implemented I-V scanner is made of locally available components and is cost-effective and convenient for research and evaluation purposes. The experiment involves covering different percentages of the area of random solar cells to simulate the effect of shading on the panel's I-V and power curves. We explain and correlate the relationship between the panel's power output and the shading coverage area in relation to soiling and bird-dropping conditions. This type of shading is different from row-to-row shading and should be carefully considered for an optimal solar farm operation.

5.1 IV Scanner Design Concept

In the I-V scanner design, we use an n-channel MOSFET (IRF540) as a non-linear variable load. The basic concept is that, for the different gate to source voltage (V_{GS}), the I-V curve of the MOSFET will change. This gives an electronically controllable, varying load for the panel. The change of I-V curve of the MOSFET will intersect at different operating points of the PV module I-V curve. Therefore, a collection of intersecting points of MOSFET and PV module I-V curve can be measured to capture the I-V characteristics curve of the PV module.

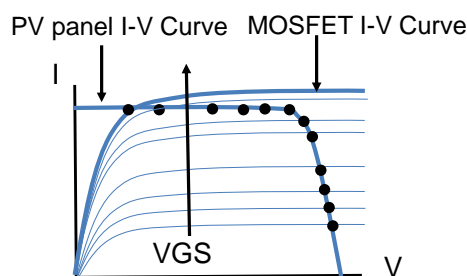


Fig. 5.1: I-V characteristics curve of MOSFET and PV module and I-V curves intersecting point.

Fig. 5.1 shows a schematic I-V characteristics curve of the MOSFET when the gate to source voltage (V_{GS}) is increased. Fig. 22 also indicates the I-V characteristics of a PV panel. When the MOSFET is used as a non-linear load for the PV panel, the I-V characteristics curve of the MOSFET intersects the specific operating points of PV module I-V characteristics as illustrated in figure. These intersecting or operating points can then be read automatically to form the module I-V characteristics.

5.2 PV Module Connection

We use 30 W PV modules (model number: SLP030-12, from Solarland) in our experiment. Each PV module has 36 solar cells interconnected in series in two strings. For conducting the experimental setup, two 30 W PV modules are connected in series. Each of the modules has 2 bypass diodes—our panel setup is therefore a 4 bypass-diode system. Fig. 5.2 (a), and (b) presents two PV modules connected in series containing 4 strings of solar cells. Each string contains one bypass diode for mitigating the effect of partial shadings. In table-5.1 we can see the technical specification of the PV modules that has been used during the experiment.

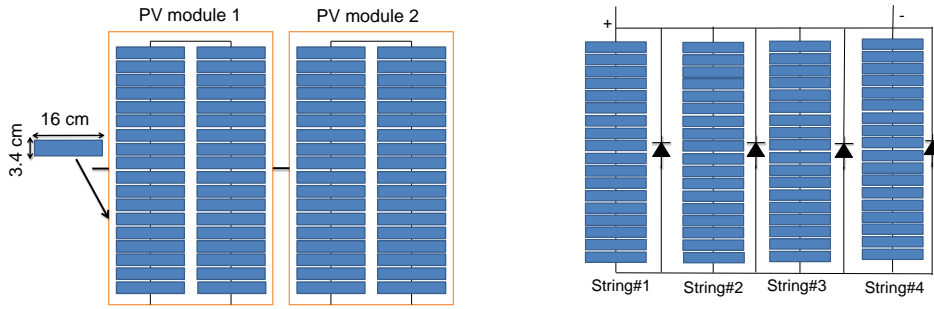


Fig. 5.2 (a) Connection of PV modules, (b) bypass diode connection in PV modules.

Table 5.1: Electrical Parameters of PV Module Specifications

| Items | Symbols | Values |
|-----------------------|-----------|--------|
| Maximum power | P_{max} | 30 W |
| Operating voltage | V_{mp} | 17.2 V |
| Operating current | I_{mp} | 1.74 A |
| Open circuit voltage | V_{OC} | 21.6 V |
| Short circuit current | I_{SC} | 1.93 A |

5.3 I-V Scanner Circuit Diagram

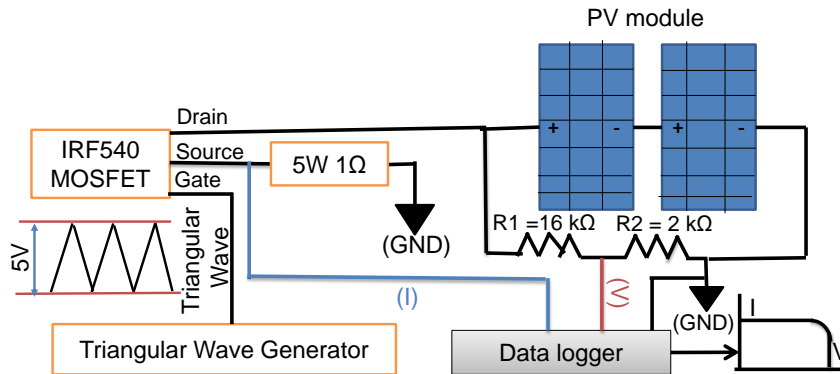


Fig. 5.3. I-V scanner schematic circuit diagram.

Fig.5.3 represents the circuit diagram of the designed I-V scanner. For switching the MOSFET IRF540, a triangular wave of 5V peak is provided to the MOSFET gate terminal from the triangular wave generator. The triangular control signal ensures that the panel I-V is automatically and repeatedly scanned. The triangular wave peak voltage is 5V and its time period is 2s. The drain terminal of the MOSFET is connected to the positive (+) terminal of the PV module. A voltage divider is used with a divider ratio of 8:1 between the PV module terminals. To ensure this ratio, $R_2 = 2k\Omega$ and $R_1 = 16k\Omega$ are chosen.

The main purpose of this voltage divider is to limit the data logger input to the analog pin of Arduino Mega within 5 V. Since the open circuit voltage of the series connected PV module is around 40 V, therefore, this 8:1 voltage divider ratio scales the voltage reading of

the PV module to 5 V. PV module voltage reading (V) is taken from the middle of the divider resistor R_1 and R_2 . During the acquisition of PV module voltage (V), the measured value is appropriately rescaled (multiplied by 9). Here, the source terminal of the MOSFET is connected to the ground through the 1Ω ceramic resistance, which reads the current (I) of the PV module through another analog pin of the data logger.

The current (I) and voltage (V) values are simultaneously measured to read each operating point. After multiple scans (multiple periods of the control triangular wave), we obtain a full I-V characteristic of the panel.

5.4 Experimental Methodology

To test partial shading conditions, we artificially cover parts of the cells in the panel setup and observe the I-V and power outputs. PV module 2 was not covered, but different cells within PV module 1 were systematically covered (partially shaded) for observing the changes in I-V characteristics curve of the PV panel setup. Table-5.2 summarizes the description of conducted experiments (labeled A, B, C, D, and E). Fig.5.4 (a) shows a solar cell area cover (%) that is used during the experiment. Here, 0% (no shading), 25%, 50%, 75%, or 100% area were covered (using black cello tape) on a cell.

Table 5.2 Description of the Conducted Partial Shading Experiment

| | | |
|---|-------|----------------------------------|
| Experiment A | expA1 | String 1, one cell 25% cover |
| | expA2 | String 1, another cell 25% cover |
| Experiment B | expB1 | 0% Cover |
| | expB2 | String 1, one cell 25% cover |
| | expB3 | String 1, one cell 50% cover |
| | expB4 | String 1, one cell 75% cover |
| | expB5 | String 1, one cell 100% cover |
| Experiment C (String 1, randomly one cell 25% fixed cover) | expC1 | String 2, one cell 25% cover |
| | expC2 | String 2, one cell 50% cover |
| | expC3 | String 2, one cell 75% cover |
| | expC4 | String 2, one cell 100% cover |
| Experiment D (String 1, randomly one cell 25% fixed cover) | expD1 | String 1, one cell 25% cover |
| | expD2 | String 1, one cell 50% cover |
| | expD3 | String 1, one cell 75% cover |
| | expD4 | String 1, one cell 100% cover |
| Experiment E | expE | String 1,2,3; 25,50, 75% cover |

Fig. 5.4(b) represents experiment B where one solar cell is picked randomly (within PV module 1, string 1) to test its change in I-V curve under 0%, 25%, 50%, 75%, and 100% area-cover conditions.

Fig. 5.4(c) illustrates the experiment C, where one solar cell (from PV module 1, string 1) was 25% covered, and another random cell (from module 1, string 2) was randomly covered from 25% to 100%.

Fig. 5.4(d) visualizes experiment D which shows one solar cell was 25% covered and another solar cell was covered from 25% to 100% — in experiment D, both the cells are within the same string (i.e., in PV module string 1). Fig-4.4(e) and (f) represent the experimental setup of the I-V scanner and an experimental example of expC4 which describes in table-5.2.

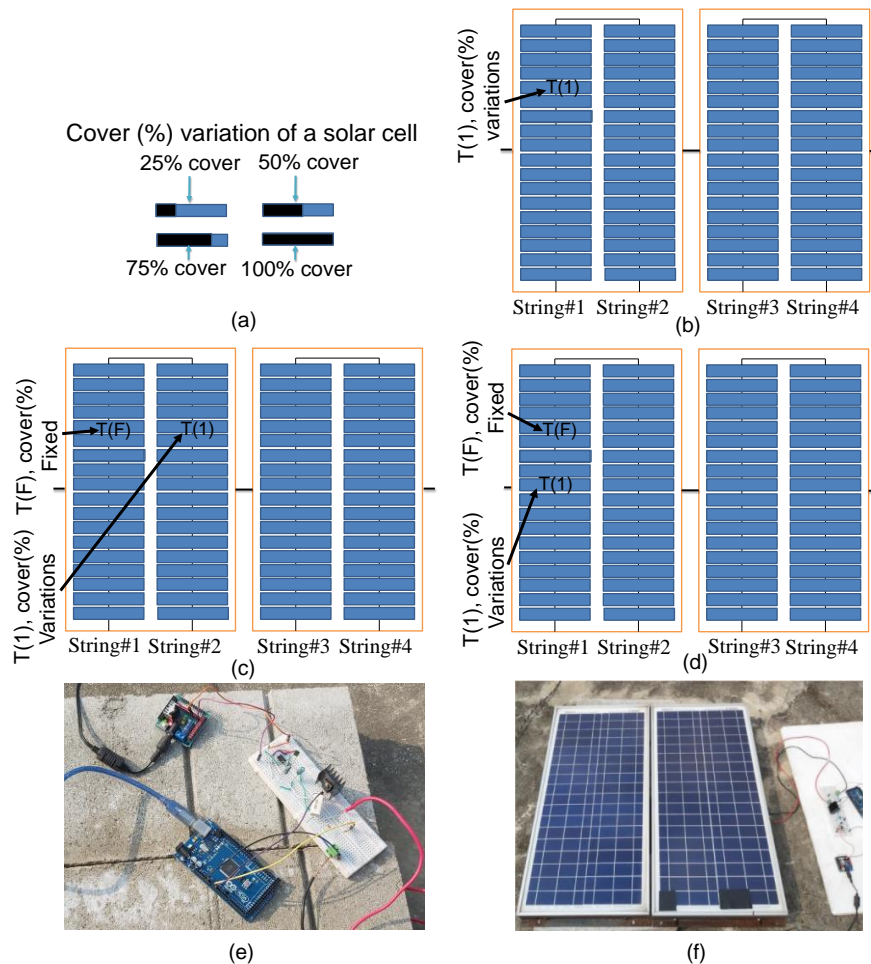


Fig. 5.4: (a) Individual solar cell cover (%) variation have been defined here. Various experiment conditions are shown: (b) experiment B: solar cell cover (%) variations in string 1, (c) experiment C: string1 fixed 25% cover, string2 individual cell cover (%) variations, (d) experiment D: string1 fixed 25% cover, string1 another cell cover (%) variations. (e) Experimental setup of I-V scanner. (f) Example of the conducted experiment, i.e. expC4 of table-II.

5.4.1 Experimental Data Analysis from Reading Data

I-V curve measurements for all the experiments listed in table-II have been done outdoors under natural lighting conditions. All the relevant measured I-V and the corresponding calculated P-V are shown in Fig. 5.5. As expected, in experiments A, B and D, the I-V has an additional step triggered by one of the bypass diodes due to shading on the same string. I-V curve in experiment C shows two additional steps correlated to activation of two separate bypass diodes in different strings. These results, however, cannot be compared as the sunlight intensity was different from one I-V reading to the other. We, therefore compare normalized I-V and P-V characteristics as discussed in the next section.

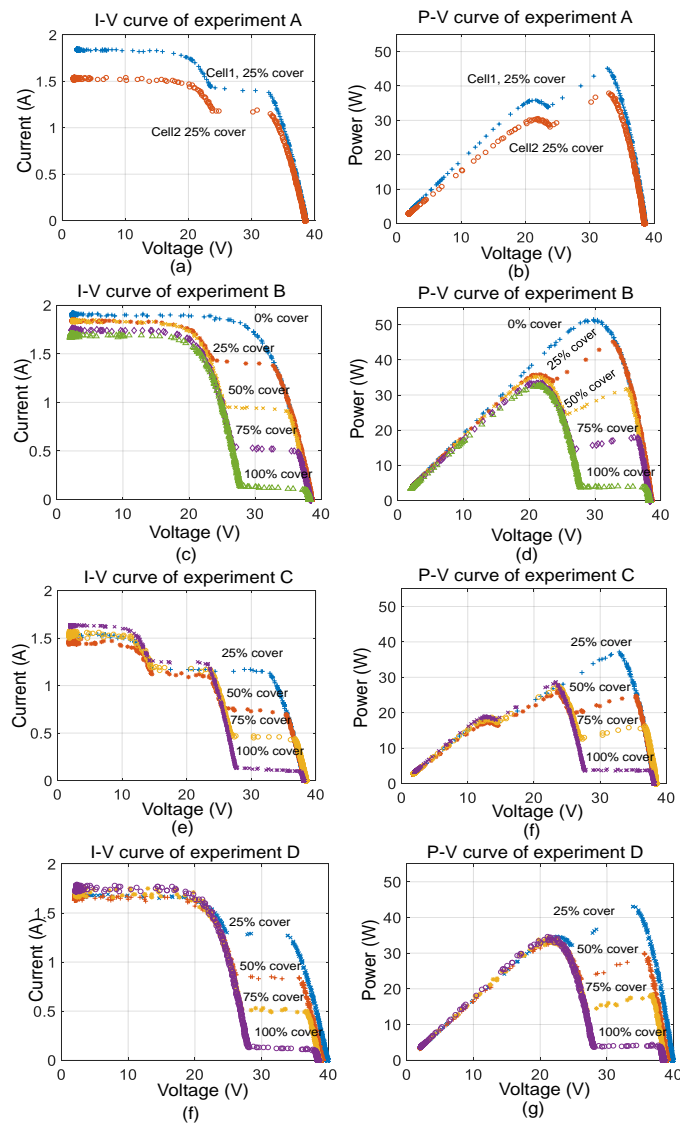


Fig. 5.5. (a) I-V curve of experiment A (a cell of string1, 25% cover; another cell of string 1, 25% cover), (b) P-V curve of experiment A, (c) I-V curve of experiment B (string 1 cell 0%, 25%, 50%, 75% and 100% cover variation), (d) P-V curve of experiment B, (e) I-V curve of experiment C (string 1, a cell 25% fixed cover, string 2 another randomly picked cell, 0%, 25%, 50%, 75%,and 100% cover variation), (f) P-V curve of experiment C, (g)) I-V curve of experiment D (string 1, a cell 25% fixed cover, string 1 another randomly picked cell, 0%, 25%, 50%, 75%, and 100% cover variation), (h) P-V curve of experiment D.

5.5 Normalized Experimental Data Analysis

For appropriate comparison of the PV panel under different shading coverage conditions, the experimental data are normalized. On a given I-V measurement, both the voltage and current have been normalized to the maximum (i.e., open circuit) voltage and the maximum current (i.e., short circuit), respectively.

Fig. 5.6(a) shows that the I-V curves from experiment A. We see here that the I-V characteristics overlap. Similarly in Fig. 5.6(b), the P-V curves of two experiments expA1 and expA2 overlap. The overlapped curves in Fig. 5.6(a) and (b) indicates that we expect the same relative lowering of output due to the same shadow coverage, irrespective of the position of the cell. Fig. 5.6(c) shows the normalized I-V curve of experiment B where, one solar cell has 25%, 50%, 75%, and 100% cover in string 1. Therefore, the bypass diode is triggered at lower voltages to maintain the same short circuit current. For 0% cover condition, we find the maximum power output as shown in Fig. 5.6(d). Fig. 5.6(d) represents the normalized power output for cell shading area coverage varied from 25% to 100%. It is observed that maximum power (P_{max}) decreases when shading changes as 0%, 25%, and 50%. The P_{max} value does not change for 50%-100% shading due to the activation of the bypass diode at the maximum power point (MPP).

Fig. 5.6(e) shows the I-V curve characteristics for all the cases of experiment C (string 1 solar cell fixed 25% cover, and another cell coverage varied from 25% to 50%, 75%, and 100%). Therefore, in all cases, string 1 bypass diode triggered at 25% of current. For exp-C1 (25%+25% shading) it seems that the coverage of the same amount area of two strings has the same impact as in exp-B with 25% shadow. From exp-C2, exp-C3, and exp-C4, it is seen that the string-2 bypass diode triggered again for 50%, 75%, and 100% coverage of the solar cell of string 2, respectively. As string-1 is also 25% shaded, the bypass diode activated MPP will also see ~25% lowered P_{max} , as observed in Fig. 5.6(f). Fig. 5.6(g) and (h) illustrates the I-V and P-V characteristics of experiment D.

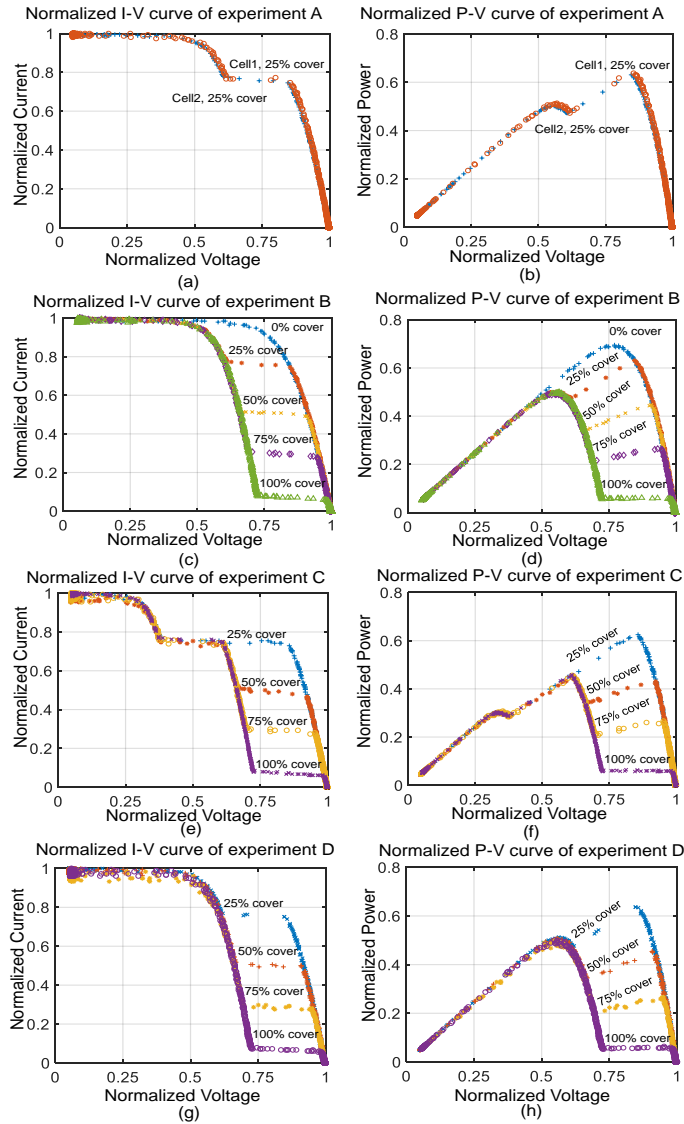


Fig. 5.6. (a) Normalized I-V curve of experiment A (a cell of string1, 25% cover; another cell of string 1, 25% cover), (b) Normalized P-V curve of experiment A, (c) Normalized I-V curve of experiment B (string 1 cell 0%, 25%, 50%, 75% and 100% cover variation), (d) Normalized P-V curve of experiment B, (e) Normalized I-V curve of experiment C (string 1, a cell 25% fixed cover, string 2 another randomly picked cell, 0%, 25%, 50%, 75% and 100% cover variation), (f) Normalized P-V curve of experiment C, (g) Normalized I-V curve of experiment D (string 1, a cell 25% fixed cover, string 1 another randomly picked cell, 0%, 25%, 50%, 75% and 100% cover variation), (h) Normalized P-V curve of experiment D.

In this experiment, one cell is 25% shaded, while shading on another cell in the same string is varied. Being under the same bypass diode, the effect of shading in two cells is dominated by the higher shadow coverage. That is why, experiment D shows identical trends as experiment B. Interestingly, we observe that the current is non-zero even when we fully cover the cell (100% coverage). This is mainly due to the following two factors: (1) the black-tape used for shading is not perfectly opaque, and (2) light scattering within the panel contributes to diffuse light collection from adjacent cell positions.

5.6 MPP Comparison of Experiment B, C, and D

Fig.5.7 indicates the comparison of maximum power (P_{max}) of experiments B, C, and D. For experiment B, from PV module1 string1, solar cell area coverage varies as 0%, 25%, 50%, 75%, and 100%. For 0% coverage, the power of the PV panel is the maximum. We observe that, up to 50% of shading, the power monotonically decreased with the percentage of shading on the solar cell. For 50% or higher cell shading P_{max} does not change.

Normalized MPP comparison of experiment B, C, and D

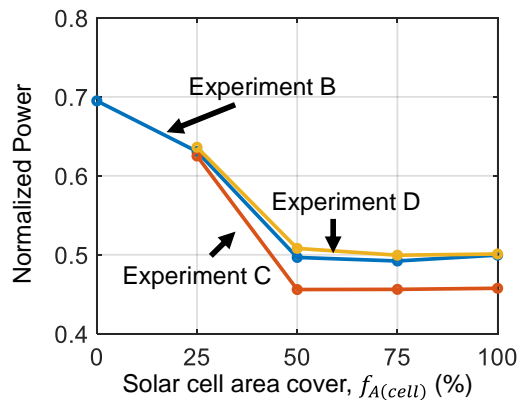


Fig. 5.7. Maximum Power Point comparison of experiment B, C, and D.

This is because the shaded string is bypassed under these high shading scenarios. This was also seen in Fig. 5.6 (P-V plots) where the MPP peak shifts to a lower voltage due to activation of bypass diodes. Experiment B and D are approximately the same due to shading on a single string, as explained in the previous subsection. For the plot for experiment C, however, we see that the P_{max} saturates at a lower value (for shading $\geq 50\%$). In this case (i.e., exp-C), after the MPP is restricted by the bypass diode, the current is also lowered at the second string due to 25% shading. That is why, the normalized power for shading of 50% or more is lower in experiment C compared to experiments B or D.

5.7 Multiple String Coverage of PV modules

Fig. 5.8(a) shows the I-V curve of experiment E where string 1 one cell was 25% covered, string 2 was 50% covered, and string 3 was 75% covered, therefore string1 diode triggered at almost 25% current, string2 diode triggered at almost 50% current, string3 diode triggered at almost 75% current. Fig. 5.8 (b) shows the P-V curve of experiment E. Here, the middle

one among the three peaks is the MPP, where all the shading effect considerations are combined.

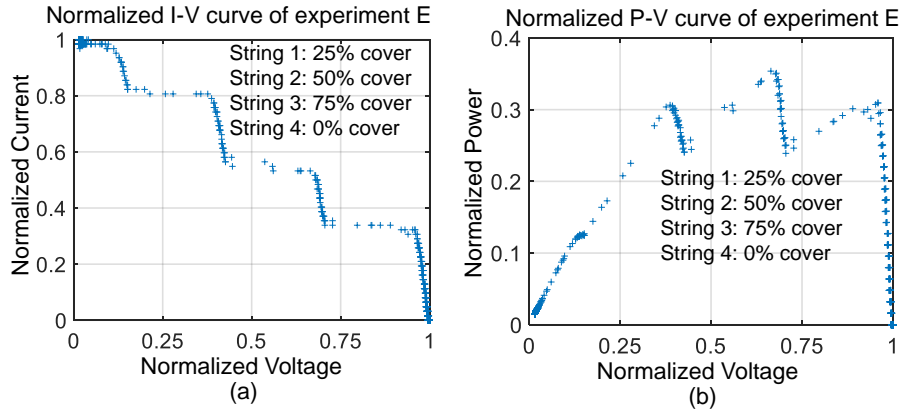


Fig. 5.8: Experiment E (a) normalized I-V curve, (b) normalized P-V curve.

5.8 Correlation with Non-Uniform Soiling and Bird-dropping

Prior literature shows that there can be three types of soiling band shape at the bottom edge of a solar panel, such as: triangular, rectangular, and transverse trapezoid [13]. Fig. 5.9(a) represents the triangular soiling band-shape which mostly covers a cell from string 1, and partially covers a cell from string 2. Fig. 5.9(b) presents the rectangular soiling band shape which covers the bottom edge of both cells of the two strings. Fig. 5.9(c) illustrates a transverse trapezoidal soiling band. Such soiling bands can remain on panels even after cleaning, especially when machine-cleaning is used. All these three scenarios can be related to our experiment-C. As we have explained earlier, the output of the system can be drastically suppressed only with partial shading of a few cells—therefore the effectiveness of cleaning should be carefully reevaluated if such soiling bands persist.

Bird-dropping can randomly shade different cells on the panel [56]. Fig. 5.9(d) represents the bird-dropping in PV panels in different strings in different portions. Effects of low to heavy bird dropping rates on panel output can therefore be correlated to all our experimental results. A combined soiling and bird-dropping scenario equivalent to our experiment-E can drastically suppress output—the desired operating output then cannot be retained until a proper cleaning intervention.

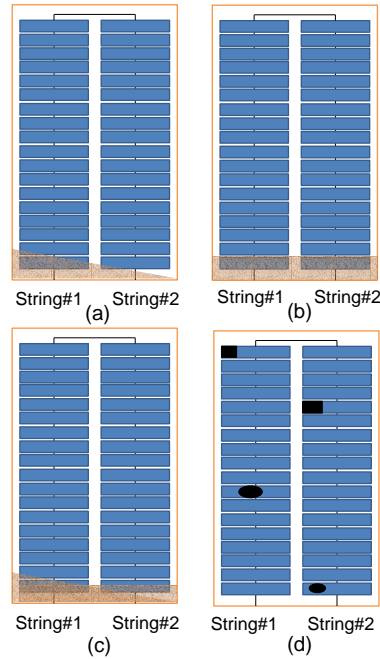


Fig. 5.9.: Soiling band schematic diagram (a) triangular, (b) rectangular, (c) transverse trapezoidal, (d) bird-dropping schematic diagram on PV panel.

5.9 Economic Analysis of Non-uniform Soiling

Non-uniform soiling drastically decreases the power generation of PV panels. Different events are responsible for the non-uniform soiling on PV panels for example bird droppings, sand storms, or snowfall. We analyzed the revenue losses due to the non-uniform soiling in a PV power plant. The designed I-V scanner has been used to observe the changes in the I-V characteristics curve of PV panels due to non-uniform soiling and shading conditions. A correlation has been done with the various shadowing condition like the bottom edge soiling condition of PV panels or bird-dropping. In a PV power plant, non-uniform soiling may occur at the edge of PV panels after cleaning intervention. Considering these, scenarios we conducted an economic analysis for determining the effect of non-uniform soiling on the revenue of PV power plants. Finally, the relations between the cleaning cycle, performance loss factor, and solar cell area coverage with respect to revenue have been also discussed in this section.

5.10 Revenue Analysis for Non-uniform Soiling

In case of uniform soiling on modules, the performance ratio, PR (unclean to clean panel output ratio) decreases daily due to dust accumulation. After a cleaning intervention, PR immediately resets to unity. The temporal characteristics of PR is saw-tooth-like with periodic cleaning—this is shown in Fig.5.10 (a). Clearly, PR is not always equal to 1 — this indicates unavoidable energy loss for any cleaning cycle t_c (>1). The cleaning cycle and its costs are chosen to maximize revenue [20]. The revenue under uniform soiling with a cleaning cycle of t_c can be written as [20]:

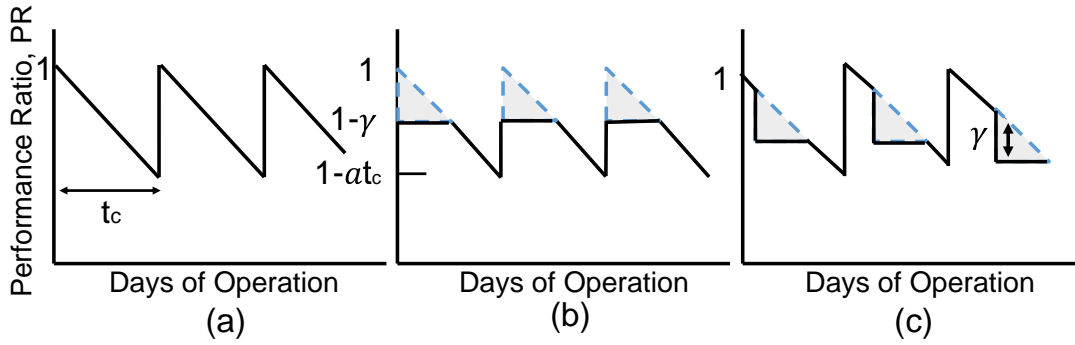


Fig. 5.10. Performance ratio versus cleaning cycle (a) without non-uniform soiling, (b) with non-uniform soiling conditions (edge soiling due to machine or manual cleaning), and (c) with non-uniform soiling conditions (bird-droppings, snowfall, sand storm)

$$\text{Rev}_U = RE_0 \left[1 - \frac{1}{2} atc - \frac{C}{RE_0} \frac{1}{t_c} \right] \quad (5.1)$$

Here, R is the tariff rate, a is the soiling rate, E_0 is the mean daily rated (i.e., clean panel) energy output, C is the cleaning cost, and t_c is the cleaning cycle.

Consider a scenario where there is always some accumulated dust (e.g., as shown in Fig. 5.10(b)) at the edges. In this case, after inefficient machine cleaning, the PR does not return to unity, see Fig. 5.10(b). We define this residual loss through the “Performance Loss (PL) Factor”, γ . With time, the module will continuously accumulate uniform dust with no reduction in PR until the rest of the module area reaches soiling-loss comparable to that at the edges. Therefore, after each inefficient cleaning cycle, the PR reaches $(1 - \gamma)$. The additional loss per cycle is marked as the shaded triangular area. The corresponding mean daily loss in PR related to this triangular area is $(\gamma^2/2a)$. A similar loss may occur due to a sudden soiling band formation due to wind, or bird dropping (see Fig. 5.10(c)).

For the uniform soiling, the PR can decrease by $\sim at_c$ at the end of a cleaning cycle. Therefore, if $\gamma > at_c$, the uniform soiling on the panel area never reaches the edge-soiling loss of γ . In such a case, the performance ratio always remains at $PR = \gamma$ showing no effect or signature of cleaning. Finally, the revenue under combined uniform and non-uniform soiling with the cleaning cycle of t_c can be written as:

$$\text{Rev}_{\text{NU}} = \begin{cases} RE_0 \left[1 - \frac{1}{2}at_c - \frac{C}{RE_0} \frac{1}{t_c} - \frac{\gamma^2}{2a} \right]; & \gamma < at_c \\ RE_0 \left(1 - \gamma - \frac{C}{RE_0} \frac{1}{t_c} \right) & ; \gamma \geq at_c \end{cases} \quad (5.2)$$

The term $(C/RE_0 t_c)$ accounts for the loss in revenue due to panel cleaning at each cleaning cycle.

Finally, the performance loss factor γ can be related to the solar cell area cover fraction ($f_{A(\text{cell})}$) from Fig.5.7. The fractional loss in ‘Normalized power’ with increasing $f_{A(\text{cell})}$ is equivalent to γ . Therefore, a second-order polynomial fit gives:

$$f_{A(\text{cell})} = -5\gamma^2 + 3.2\gamma \quad (5.3)$$

Equations (5.2) and (5.3) relate the revenue (Rev_{NU}) to the solar cell area cover fraction ($f_{A(\text{cell})}$) due to non-uniform soiling in presence of constant uniform soiling (rate: a).

Fig. 5.11 and 5.12 show the normalized revenue and the revenue in the presence of uniform non-uniform soiling. Normalized revenue is the dust-affected revenue normalized to the soiling-free revenue of a solar farm. The revenue, of course, considers the reduction in cash-inflow due to costs incurred by periodic panel cleaning. In our calculations, we assume values relevant to South Asia: $R = 0.0895$ USD/kWh, $E_0 = .1123$ kWh/day, $C = 0.03$ USD/kWh/Wp, $a=0.8\%$ /day [4], [11].

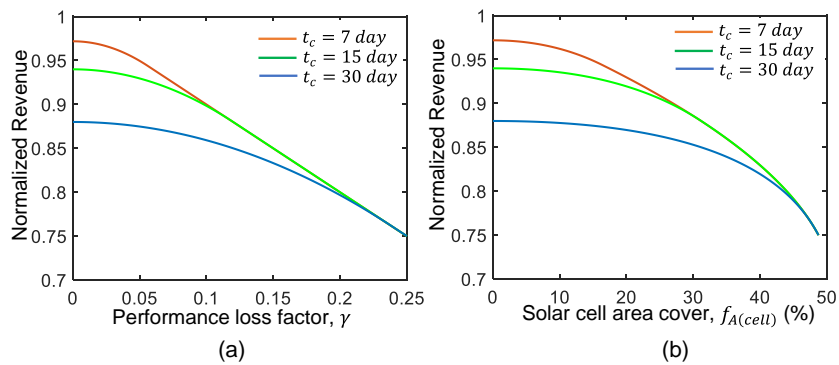


Fig. 5.11. Relationship between (a) normalized revenue and decreasing factor of performance ratio (γ) (b) normalized revenue and covered area (%) due to non-uniform soiling.

With, $f_{A(cell)} = 0$ (i.e., $\gamma = 0$), there is no non-uniform soiling. However, as shown in Fig. 5.11, due to natural uniform soil accumulation the normalized revenue f_R is 97%, 94%, and 88% for cleaning cycles of $t_C = 7, 15,$ and 30 days, respectively. This means we will lose 3%, 6%, and 12% of the rated clean-panel revenue during these cleaning cycles—it is impossible to reduce the revenue loss to zero in presence of soiling [4]. The corresponding revenue values are shown in fig. 5.12. With increased non-uniform soiling (e.g., due to inefficient cleaning), $f_{A(cell)} > 0$ and the revenue decreases further (as explained in eqn. (5.3)).

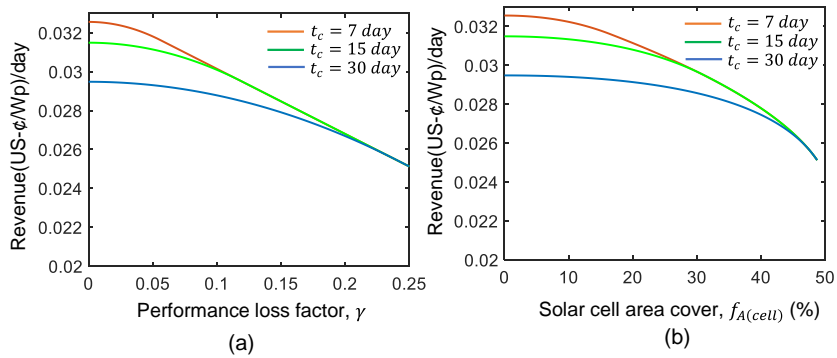


Fig. 5.12. Relationship between (a) revenue and decreasing factor of performance ratio (γ) (b) revenue and covered area (%) due to non-uniform soiling.

The non-uniform soiling, i.e., $f_{A(cell)} > 0$ can have a strong reduction in revenue. Interestingly, for $f_{A(cell)} > 25\%$ cleaning cycles of 7 and 15 days result in similarly reduced revenues—the loss is $>10\%$. This extraordinarily high loss will persist unless the panels and their edges are appropriately cleaned. In the unlikely case when $f_{A(cell)} > 45\%$, $t_C = 7, 15,$ or 30 days result in the same $>20\%$ loss in revenue.

CHAPTER 6

CONCLUSIONS

This chapter summarizes the research work on the techno-economic analysis of uniform and non-uniform soiling for both mono-facial and bifacial setups. It also discusses the limitations of the research work and the future work that can be done to further explore this field.

6.1 Monofacial PV Setup Experiment

In this research, we had experimented in three months January, February, and March of 2022. We determined the soiling rate for monofacial panels tilted at 0° , 10° , 20° , 30° , 60° , and 90° . To determine the performance ratio and soiling rates in South Asia, we experimentally assess the outputs of clean and weekly clean, and monthly clean panels at these tilts (Dhaka, Bangladesh). Finally, we used these average soiling rates to evaluate the economic analysis for these monofacial PV panels. We also showed the revenue comparison among always clean, weekly clean, and monthly clean. The most interesting part is that from the soiling average we have linearly fitted the curve and determined a formula, by using which we can predict the soiling rate of a specific location.

The average soiling rates for monthly clean panel are 1.13, 1.07, 0.95, 0.82, 0.44, and 0.019%/day respectively. The corresponding predicted optimal cleaning cycles are 4, 4, 4, 6, and 30 days. During the economic analysis, we found that 30° weekly clean panel shows the maximum revenue during the experimental period. For all tilt angles weekly clean panel shows the maximum revenue than the monthly clean panel.

6.2 Bifacial PV Setup Experiment

In this work, we have presented a techno-economic analysis of the effect of soiling on monofacial and bifacial panels tilted at 0° , 20° , and 30° . We experimentally measure the outputs of clean and unclean panels at these tilts to calculate the performance ratio and soiling rates in South Asia (Dhaka, Bangladesh). We finally present a model and its predictions of cleaning cycle-dependent revenue. In winter, we experimentally observe soiling rates of 1.058, 0.753, and 0.687 %/day at the front faces of the 0° , 20° , and 30° tilted

bifacial panel setup, respectively. The corresponding predicted optimal cleaning cycles are 5, 5, and 6 days. The soiling on the back faces was negligible. Our numerical analysis shows that optimal cleaning increases the revenue by 5.5-8% (or 7.5-10%) for bifacial (or monofacial) panels compared to monthly cleaning.

Finally, the unclean (UC) panels underwent five rain events (natural cleaning) within the two-month experiment. Yet, the optimally cleaned (OC) panels are predicted to have higher revenue (cash-inflow minus costs) even with the higher net cleaning expenditures.

6.3 Non-uniform soiling and Economic Analysis

6.3.1 Designing I-V Scanner and Conducting Experiment

We have presented a simple design of an I-V scanner along with its implementation technique in this paper. Using this I-V scanner, we measured and analyzed the effects of partial shading on a 4-bypass diode PV panel system. The partial shading experiments were designed to understand the effects in the case of soil accumulation on panel edges or bird droppings. Such partial shading conditions are fundamentally different from the more commonly studied row-to-row shadings. Through our experiments, we have observed and explained how output can degrade with partial shading on single or multiple cells within the same string. In such cases, only one bypass diode may be active at MPP at high shading. Shading on only a few cells (e.g., in the case of bird droppings) in multiple strings can drastically reduce output.

Finally, the maximum output power correlation with the solar cell coverage area (%) is also shown to better understand the effect of non-uniformly accumulated soiling on the bottom edge solar cell PV module. More importantly, such soiling bands may remain after machine cleaning—therefore, the large panel arrays may continue to underperform even after cleaning. Based on the understanding of this paper, the edge soiling and bird-dropping cases should be more carefully addressed in a large array of panels in solar farms.

6.4 Summary of Techno-Economic Analysis under Uniform Soiling Conditions

We did the economic analysis in two parts: (a) Techno-economic analysis using data from the experiment, and (b) Revenue and cleaning cycle prediction using numerical analysis.

We did the economic analysis for both monofacial and bifacial PV setups. The techno-economic analysis showed that the soiling free panel had the highest revenue because we did not deduct the cleaning cost from the revenue. The soiling free panel and the daily cleaned panel produced the same amount of energy, but the daily cleaned panel had the lowest revenue because of the high cleaning cost. The daily cleaned panel also had lower revenue than the weekly and monthly cleaned panels. In reality, a soiling free panel is not possible, so we cannot get the maximum revenue by cleaning the PV panel every day. On the other hand, if we clean the PV panel once a month, we will lose revenue because of the energy loss due to soiling. Therefore, there is an optimum cleaning cycle that balances between revenue and cleaning cost.

The numerical analysis showed that for PV panels with tilt angles from 0° to 60° , the optimum cleaning cycle is 4 to 6 days. The experiment results also showed that for a 7-day cleaning cycle, we got more revenue than for a daily or a monthly cleaning cycle. So, to get the maximum revenue from a PV power plant, we can conclude that the optimum cleaning cycle is the best option.

6.5 Summary of Techno-Economic Analysis under Non-uniform Soiling Conditions

We modeled a numerical analysis for evaluating techno-economic analysis where the non-uniform soiling conditions are considered. The relationship of revenue between the performance loss factor and area cover (%) due to non-uniform soiling is also shown in this study.

During the experiment, we found the I-V characteristics curve of a PV panel changes abruptly concerning the different shadowing conditions. In a string of a PV panel when around 50% shadow occurred then the bypass diode of that string is triggered therefore then the output power does not change even if the area coverage increases. We have found that the cleaning cycle has a significant influence on the non-uniform soiling effect. In uniform soiling conditions for 7 days cleaning cycle, the normalized revenue becomes 97%, and for

the cleaning cycle of 15 and 30 days, the revenue becomes 94% and 88% respectively. Surprisingly for cleaning cycles 7 and 15 days, if the area of non-uniform soiling on a solar cell is greater than 25% then the decrease of revenue for both cleaning cycle become the same. For cleaning cycles of 7, 15, and 30 days, the revenue decrease for all cleaning cycles is the same if the non-uniform soiling area on a solar cell exceeds 45%. Therefore, in these rated cleaning cycles it is impossible to avoid the effect of non-uniform soiling on the PV panels. From the study, we found the lower the cleaning cycle the lower the loss due to non-uniform soiling. Non-uniform soiling on PV panels can reduce the power generation of a PV panel drastically. The effect of non-uniform soiling cannot be mitigated until the cleaning intervention is performed. Therefore, when engineers design the PV power plant, should address the condition of non-uniform soiling in PV panels on different cleaning cycles for ensuring maximum revenue.

6.6 Implications of this Thesis

The aim of this thesis is to measure the soiling rate, determine the optimum cleaning cycle for different tilt angles of solar panels. This study also examines the impact of uniform and non-uniform soiling on solar panel performance. This study can help the PV power plants in Bangladesh to maximize their revenue by balancing revenue and net cleaning cost. We propose the optimum cleaning cycle for various tilt angles and suggest that PV power plants follow it to ensure maximum revenue. We developed and built a low-cost and portable I-V scanner that can be easily used by PV power plants to detect non-uniform soiling conditions of solar panels. This thesis can help PV power plants to reduce the energy loss due to uniform and non-uniform soiling. If PV power plant can generate electricity efficiently and profitably, then this result can attract more investment in sustainable energy sector. This can help to meet the country's energy demand and reduce the reliance on fossil fuels. Installing more PV power plants and using them efficiently to generate electricity can help to address the energy crisis in this country.

6.7 Limitations of the Research Work

No research work is perfect and this thesis paper is no exception. It is the result of many months of hard work, research and analysis. We achieved all the objectives of this research, but we also faced some limitations during the experiments. We mention them in the following section.

- i. A full year data and its analysis would have given a more comprehensive understanding of soiling-cleaning in Bangladesh. Due to limited time and resource, we only focused on the dry season. Nonetheless, the estimation from the dry season is a very good estimate of soiling and cleaning in our country as the panels would stay clean in the rainy season due to regular rainfall.
- ii. We conducted the experiment for only one location, it would have been good if we could conduct the experiment for multiple locations.
- iii. It would have been fine if we could assess the air quality index data of site for analyzing the economic analysis. But we got a basic idea about the weather pattern and soiling physics for our location.
- iv. We understood there are lots of scopes to investigate the effect of Non-uniform soiling conditions on solar panels. We could not perform the statistical analysis of the PV panel performance due to non-uniform soiling, because of our limited time and resources.

6.8 Future Work of the Research

The research we did definitely provides a comprehensive picture of the soiling effect on PV panels. With these scenarios, which account for both non-uniform and uniform soiling events, we are delighted with our results. Where each analysis is compared to previous research. However, we proposed some further work for the project that we would carry out if we ever had enough resources.

- i. In the future, for a better understanding the soiling physics, one can observe the angle dependence of the soiling rate more accurately by considering the data reading in every hour or minute by minute.
- ii. One can also try to conduct the experiment in different locations of Bangladesh.
- iii. For observing the non-uniform soiling more clearly large PV panels (300-watt) for the purpose of the experiment can be used.

REFERENCES

- [1] A. Allouhi, S. Rehman, M. S. Buker, and Z. Said, “Up-to-date literature review on Solar PV systems: Technology progress, market status and R&D,” *Journal of Cleaner Production*, vol. 362, p. 132339, Aug. 2022, doi: 10.1016/j.jclepro.2022.132339.
- [2] “Renewables 2021 – Analysis,” *IEA*. <https://www.iea.org/reports/renewables-2021> (accessed Feb. 23, 2023).
- [3] “Renewables 2019 – Analysis,” *IEA*. <https://www.iea.org/reports/renewables-2019> (accessed Dec. 28, 2021).
- [4] Md. M. H. Mithhu, T. A. Rima, and M. R. Khan, “Global analysis of optimal cleaning cycle and profit of soiling affected solar panels,” *Applied Energy*, vol. 285, p. 116436, Mar. 2021, doi: 10.1016/j.apenergy.2021.116436.
- [5] Jim Joseph John, “Characterization of Soiling Loss on Photovoltaic Modules, and Development of a Novel Cleaning System,” *Doctor thesis, Department of Electrical Engineering, Indian Institute of Technology, Bombay.*, 2015.
- [6] A. Sayyah, M. N. Horenstein, and M. K. Mazumder, “Energy yield loss caused by dust deposition on photovoltaic panels,” *Solar Energy*, vol. 107, pp. 576–604, Sep. 2014, doi: 10.1016/j.solener.2014.05.030.
- [7] R. Jones *et al.*, “Optimized Cleaning Cost and Schedule Based on Observed Soiling Conditions for Photovoltaic Plants in Central Saudi Arabia,” *IEEE Journal of Photovoltaics*, pp. 1–9, Mar. 2016, doi: 10.1109/JPHOTOV.2016.2535308.
- [8] J. G. Bessa, L. Micheli, F. Almonacid, and E. F. Fernández, “Monitoring photovoltaic soiling: assessment, challenges, and perspectives of current and potential strategies,” *iScience*, vol. 24, no. 3, p. 102165, Mar. 2021, doi: 10.1016/j.isci.2021.102165.
- [9] “EU Market Outlook for Solar Power 2021-2025 - SolarPower Europe.” <https://www.solarpowereurope.org/insights/market-outlooks/market-outlook> (accessed Sep. 20, 2022).
- [10] M. R. Maghami, H. Hizam, C. Gomes, M. A. Radzi, M. I. Rezadad, and S. Hajighorbani, “Power loss due to soiling on solar panel: A review,” *Renewable and Sustainable Energy Reviews*, vol. 59, pp. 1307–1316, Jun. 2016, doi: 10.1016/j.rser.2016.01.044.
- [11] J. B. Jahangir *et al.*, “Prediction of Yield, Soiling Loss, and Cleaning Cycle: A Case Study in South Asian Highly Construction-Active Urban Zone,” in *2020 47th IEEE*

- Photovoltaic Specialists Conference (PVSC)*, Jun. 2020, pp. 1371–1374. doi: 10.1109/PVSC45281.2020.9300606.
- [12] R. Xu, K. Ni, Y. Hu, J. Si, H. Wen, and D. Yu, “Analysis of the optimum tilt angle for a soiled PV panel,” *Energy Conversion and Management*, vol. 148, pp. 100–109, Sep. 2017, doi: 10.1016/j.enconman.2017.05.058.
- [13] Y.-Q. Cui, J.-H. Xiao, J.-L. Xiang, and J.-H. Sun, “Characterization of Soiling Bands on the Bottom Edges of PV Modules,” *Frontiers in Energy Research*, vol. 9, p. 145, 2021, doi: 10.3389/fenrg.2021.665411.
- [14] L. Fialho, R. Melicio, V. M. F. Mendes, J. Figueiredo, and M. Collares-Pereira, “Effect of Shading on Series Solar Modules: Simulation and Experimental Results,” *Procedia Technology*, vol. 17, pp. 295–302, Jan. 2014, doi: 10.1016/j.protcy.2014.10.240.
- [15] L. L. Kazmerski *et al.*, “Interrelationships Among Non-Uniform Soiling Distributions and PV Module Performance Parameters, Climate Conditions, and Soiling Particle and Module Surface Properties,” in *2017 IEEE 44th Photovoltaic Specialist Conference (PVSC)*, Jun. 2017, pp. 2307–2311. doi: 10.1109/PVSC.2017.8366584.
- [16] J. G. Bessa, L. Micheli, F. Almonacid, and E. F. Fernández, “Monitoring photovoltaic soiling: assessment, challenges, and perspectives of current and potential strategies,” *iScience*, vol. 24, no. 3, p. 102165, Mar. 2021, doi: 10.1016/j.isci.2021.102165.
- [17] E. Lorenzo, R. Moretón, and I. Luque, “Dust effects on PV array performance: in-field observations with non-uniform patterns,” *Progress in Photovoltaics: Research and Applications*, vol. 22, no. 6, pp. 666–670, 2014, doi: 10.1002/pip.2348.
- [18] B. Guo, W. Javed, B. W. Figgis, and T. Mirza, “Effect of dust and weather conditions on photovoltaic performance in Doha, Qatar,” in *2015 First Workshop on Smart Grid and Renewable Energy (SGRE)*, Mar. 2015, pp. 1–6. doi: 10.1109/SGRE.2015.7208718.
- [19] M. Gostein, B. Littmann, J. Caron, and L. Dunn, “Comparing PV power plant soiling measurements extracted from PV module irradiance and power measurements,” presented at the Conference Record of the IEEE Photovoltaic Specialists Conference, Jun. 2013, pp. 3004–3009. doi: 10.1109/PVSC.2013.6745094.
- [20] M. D. Yandt, J. P. D. Cook, M. Kelly, H. Schriemer, and K. Hinzer, “Dynamic Real-Time I–V Curve Measurement System for Indoor/Outdoor Characterization of Photovoltaic Cells and Modules,” *IEEE Journal of Photovoltaics*, vol. 5, no. 1, pp. 337–343, Jan. 2015, doi: 10.1109/JPHOTOV.2014.2366690.

- [21] T. A. Pereira, L. Schmitz, W. M. dos Santos, D. C. Martins, and R. F. Coelho, “Design of a Portable Photovoltaic I–V Curve Tracer Based on the DC–DC Converter Method,” *IEEE Journal of Photovoltaics*, vol. 11, no. 2, pp. 552–560, Mar. 2021, doi: 10.1109/JPHOTOV.2021.3049903.
- [22] “Solar Park | National Database of Renewable Energy, SREDA.” <http://www.renewableenergy.gov.bd/index.php?id=1&i=1> (accessed Sep. 18, 2022).
- [23] M. Hasan and A. Rahman, “Target to generate 4,100MW by 2030,” *The Daily Star*, Oct. 31, 2021. <https://www.thedailystar.net/business/economy/news/target-generate-4100mw-2030-2210291> (accessed Sep. 18, 2022).
- [24] Md. N. Alam, S. Aziz, R. Karim, and S. A. Chowdhury, “Impact of Solar PV Panel Cleaning Frequency on the Performance of a Rooftop Solar PV Plant,” in *2021 6th International Conference on Development in Renewable Energy Technology (ICDRET)*, Dec. 2021, pp. 1–4. doi: 10.1109/ICDRET54330.2021.9752681.
- [25] “How to clean solar panels without water,” *MIT News | Massachusetts Institute of Technology*, Mar. 11, 2022. <https://news.mit.edu/2022/solar-panels-dust-magnets-0311> (accessed Mar. 09, 2023).
- [26] “International Technology Roadmap for Photovoltaic (ITRPV) - vdma.org - VDMA.” <https://www.vdma.org/international-technology-roadmap-photovoltaic> (accessed Feb. 28, 2022).
- [27] M. T. Patel, M. R. Khan, X. Sun, and M. A. Alam, “A worldwide cost-based design and optimization of tilted bifacial solar farms,” *Applied Energy*, vol. 247, pp. 467–479, Aug. 2019, doi: 10.1016/j.apenergy.2019.03.150.
- [28] U. A. Yusufoglu, T. M. Pletzer, L. J. Koduvelikulathu, C. Comparotto, R. Kopecek, and H. Kurz, “Analysis of the Annual Performance of Bifacial Modules and Optimization Methods,” *IEEE Journal of Photovoltaics*, vol. 5, no. 1, pp. 320–328, Jan. 2015, doi: 10.1109/JPHOTOV.2014.2364406.
- [29] “Statistical Review of World Energy | Energy economics | Home.” <https://www.bp.com/en/global/corporate/energy-economics/statistical-review-of-world-energy.html> (accessed Feb. 27, 2022).
- [30] “Future of Photovoltaic.” <https://www.irena.org/publications/2019/Nov/Future-of-Solar-Photovoltaic> (accessed Jan. 08, 2023).
- [31] K. K. Ilse, B. W. Figgis, V. Naumann, C. Hagendorf, and J. Bagdahn, “Fundamentals of soiling processes on photovoltaic modules,” *Renewable and Sustainable Energy Reviews*, vol. 98, pp. 239–254, Dec. 2018, doi: 10.1016/j.rser.2018.09.015.

- [32] M. G. Deceglie, L. Micheli, and M. Muller, “Quantifying Soiling Loss Directly From PV Yield,” *IEEE Journal of Photovoltaics*, vol. 8, no. 2, pp. 547–551, Mar. 2018, doi: 10.1109/JPHOTOV.2017.2784682.
- [33] A. Ullah, A. Amin, T. Haider, M. Saleem, and N. Z. Butt, “Investigation of soiling effects, dust chemistry and optimum cleaning schedule for PV modules in Lahore, Pakistan,” *Renewable Energy*, vol. 150, no. C, pp. 456–468, 2020, Accessed: Jan. 08, 2023. [Online]. Available: <https://ideas.repec.org//a/eee/renene/v150y2020icp456-468.html>
- [34] Y. N. Chanchangi, A. Ghosh, S. Sundaram, and T. K. Mallick, “Angular dependencies of soiling loss on photovoltaic performance in Nigeria,” *Solar Energy*, vol. 225, pp. 108–121, Sep. 2021, doi: 10.1016/j.solener.2021.07.001.
- [35] E. G. Luque, F. Antonanzas-Torres, and R. Escobar, “Effect of soiling in bifacial PV modules and cleaning schedule optimization,” *Energy Conversion and Management*, vol. 174, pp. 615–625, Oct. 2018, doi: 10.1016/j.enconman.2018.08.065.
- [36] S. C. S. Costa, A. S. A. C. Diniz, and L. L. Kazmerski, “Solar energy dust and soiling R&D progress: Literature review update for 2016,” *Renewable and Sustainable Energy Reviews*, vol. 82, pp. 2504–2536, Feb. 2018, doi: 10.1016/j.rser.2017.09.015.
- [37] C. Schill, S. Brachmann, and M. Koehl, “Impact of soiling on IV-curves and efficiency of PV-modules,” *Solar Energy*, vol. 112, pp. 259–262, Feb. 2015, doi: 10.1016/j.solener.2014.12.003.
- [38] Matteo Dal Molin, “Experimental Analysis of the Impact of Soiling on Photovoltaic Modules Performance,” *Master’s thesis. Milan: Politecnico di Milano*, 2018.
- [39] H. Qasem, T. R. Betts, H. Müllejans, H. AlBusairi, and R. Gottschalg, “Dust-induced shading on photovoltaic modules,” *Progress in Photovoltaics: Research and Applications*, vol. 22, no. 2, pp. 218–226, 2014, doi: 10.1002/pip.2230.
- [40] A. Karthick, M. Manokar Athikesavan, M. K. Pasupathi, N. Manoj Kumar, S. S. Chopra, and A. Ghosh, “Investigation of Inorganic Phase Change Material for a Semi-Transparent Photovoltaic (STPV) Module,” *Energies*, vol. 13, no. 14, Art. no. 14, Jan. 2020, doi: 10.3390/en13143582.
- [41] A. AlDowsari, R. Bkayrat, H. AlZain, and T. Shahin, “Best practices for mitigating soiling risk on PV power plants,” in *2014 Saudi Arabia Smart Grid Conference (SASG)*, Dec. 2014, pp. 1–6. doi: 10.1109/SASG.2014.7274291.

- [42] G. Cipriani, A. D’Amico, S. Guarino, D. Manno, M. Traverso, and V. Di Dio, “Convolutional Neural Network for Dust and Hotspot Classification in PV Modules,” *Energies*, vol. 13, no. 23, Art. no. 23, Jan. 2020, doi: 10.3390/en13236357.
- [43] P. Manganiello, M. Balato, and M. Vitelli, “A Survey on Mismatching and Aging of PV Modules: The Closed Loop,” *IEEE Transactions on Industrial Electronics*, vol. 62, no. 11, pp. 7276–7286, Nov. 2015, doi: 10.1109/TIE.2015.2418731.
- [44] M. Gökdağ, M. Akbaba, and O. Gulbudak, “Switched-capacitor converter for PV modules under partial shading and mismatch conditions,” *Solar Energy*, vol. 170, pp. 723–731, Aug. 2018, doi: 10.1016/j.solener.2018.06.010.
- [45] A. Mohapatra, B. Nayak, P. Das, and K. B. Mohanty, “A review on MPPT techniques of PV system under partial shading condition,” *Renewable and Sustainable Energy Reviews*, vol. 80, pp. 854–867, Dec. 2017, doi: 10.1016/j.rser.2017.05.083.
- [46] “The view-factor effect shaping of IV characteristics-MedSci.cn.” https://www.medsci.cn/sci/show_paper.asp?id=38ea2118a2c05e8d (accessed Aug. 25, 2021).
- [47] S. Gallardo-Saavedra and B. Karlsson, “Simulation, validation and analysis of shading effects on a PV system,” *Solar Energy*, vol. 170, pp. 828–839, Aug. 2018, doi: 10.1016/j.solener.2018.06.035.
- [48] S. A. Sulaiman, H. H. Hussain, N. S. H. N. Leh, and M. S. I. Razali, “Effects of Dust on the Performance of PV Panels,” *International Journal of Mechanical and Mechatronics Engineering*, vol. 5, no. 10, pp. 2021–2026, Oct. 2011, Accessed: Mar. 14, 2022. [Online]. Available: <https://publications.waset.org/10305/effects-of-dust-on-the-performance-of-pv-panels>
- [49] E. Pigueiras, R. Moretón, and I. Luque, “Dust effects on PV array performance: In-field observations with non-uniform patterns,” *Progress in Photovoltaics: Research and Applications*, vol. 22, Jun. 2014, doi: 10.1002/pip.2348.
- [50] M. Gostein, T. Düster, and C. Thuman, “Accurately measuring PV soiling losses with soiling station employing module power measurements,” in *2015 IEEE 42nd Photovoltaic Specialist Conference (PVSC)*, Jun. 2015, pp. 1–4. doi: 10.1109/PVSC.2015.7355993.
- [51] A. Kimber, L. Mitchell, S. Nogradi, and H. Wenger, “The Effect of Soiling on Large Grid-Connected Photovoltaic Systems in California and the Southwest Region of the United States,” in *2006 IEEE 4th World Conference on Photovoltaic Energy Conference*, May 2006, pp. 2391–2395. doi: 10.1109/WCPEC.2006.279690.

- [52] V. Gupta, M. Sharma, R. K. Pachauri, and K. N. Dinesh Babu, “Comprehensive review on effect of dust on solar photovoltaic system and mitigation techniques,” *Solar Energy*, vol. 191, pp. 596–622, Oct. 2019, doi: 10.1016/j.solener.2019.08.079.
- [53] Y. N. Chanchangi, A. Ghosh, S. Sundaram, and T. K. Mallick, “Dust and PV Performance in Nigeria: A review,” *Renewable and Sustainable Energy Reviews*, vol. 121, p. 109704, Apr. 2020, doi: 10.1016/j.rser.2020.109704.
- [54] X. Sun, M. R. Khan, C. Deline, and M. A. Alam, “Optimization and performance of bifacial solar modules: A global perspective,” *Applied Energy*, vol. 212, pp. 1601–1610, Feb. 2018, doi: 10.1016/j.apenergy.2017.12.041.
- [55] B. Zhao, “Purdue University Bifacial Module Calculator (PUB),” 2018, doi: <https://doi.org/10.21981/19PR-0W68>.
- [56] A. Sisodia and R. Mathur, “Impact of bird dropping deposition on solar photovoltaic module performance: a systematic study in Western Rajasthan,” *Environmental Science and Pollution Research*, vol. 26, Oct. 2019, doi: 10.1007/s11356-019-06100-2.

LIST OF PUBLICATIONS

Conference Papers: (Peer-Reviewed)

1. D. Islam, M. A. Islam, and M. R. Khan, "Design of I-V Scanner to Analyze the Effects of Partial Shading due to Soiling and Bird-dropping on PV Panels," in 2021 5th International Conference on Electrical Engineering and Information Communication Technology (ICEEICT), Nov. 2021, pp. 1–6. doi: 10.1109/ICEEICT53905.2021.9667805.
2. D. Islam, M. A. Islam, R. N. Sajjad, and M. R. Khan, "A Techno-Economic Analysis of Bifacial Panels Under Soiling in South-Asian Urban Area," in 2022 IEEE Region 10 Symposium (TENSYP), Jul. 2022, pp. 1–5. doi: 10.1109/TENSYP54529.2022.9864510.

Journal Papers: (Peer-Reviewed)

1. D. Islam, M. A. Islam, and M. R. Khan, "Effect of non-uniform soiling on solar panel output and revenue analyzed through a controlled experiment by using a designed I-V scanner," MIST International Journal of Science and Technology, vol. 10, pp. 21–28, December 2022, doi: [https://doi.org/10.47981/j.mijst.10\(02\)2022.346\(21-28\)](https://doi.org/10.47981/j.mijst.10(02)2022.346(21-28)).